

AD

Influence of the proton concentration on the properties of the LiNbO_3 and LiTaO_3 crystals

Final report
by
M.P. DE MICHELI
July 1997

United States Army

EUROPEAN RESEARCH OFFICE OF THE U.S. ARMY
London England

CONTRACT NUMBER : N68171-96-C-9040
R&D 7774-EE-01

Laboratoire de Physique de la Matière Condensée
CNRS
Parc VALROSE, 06108 NICE CEDEX2, FRANCE

QC QUALITY INSPECTED 4

Approved for Public Release, distribution unlimited.

19970911 080

REPORT DOCUMENTATION PAGE			
1. AGENCY USE ONLY	2. REPORT DATE 07/14/97	3. REPORT TYPE AND DATES COVERED Final report : July 96 - July 97	
4. TITLE : Influence of the proton concentration on the properties of the LiNbO ₃ and LiTaO ₃ crystals			5. FUNDING NUMBERS
6. AUTHOR : M.P. DE MICHELI			
7. PERFORMING ORGANIZATION NAMES AND ADDRESSES Laboratories de Physique de la Matière Condensée Parc Valrose, 06108 NICE Cedex 2 , FRANCE			8. PERFORMING ORGANIZATION REPORT NUMBER
9. SPONSORING, MONITORING AGENCY NAMES AND ADDRESSES			10. SPONSORING, MONITORING AGENCY REPORT NUMBER
11. SUPPLEMENTARY NOTES			
12A. DISTRIBUTION / AVAILABILITY STATEMENT Approved for Public Release, distribution unlimited.			12B. DISTRIBUTION CODE
13. ABSTRACT During this first year, a set of optical waveguides has been realized on LiNbO ₃ , using different PE recipes. They have been characterized optically and rocking curves as well as SIMS measurements have been performed. Some correlation have been evidenced and we are working on more sophisticated details. Influence of the waveguide fabrication process on the nonlinearity and on the poling parameters have also been observed. Experiments are in progress in order to be able to have a more quantitative approach.			
14. SUBJECT TERMS Optical waveguides, Nonlinear Optics, Lithium niobate, Proton exchange, periodic poling.			15. NUMBER OF PAGES
			16. PRICE CODE
17. SECURITY CLASSIFICATION OF THE REPORT	18. SECURITY CLASSIFICATION OF THIS PAGE	19. SECURITY CLASSIFICATION OF ABSTRACT	20. LIMITATION OF ABSTRACT

Influence of the proton concentration ...	3
---	---

Index

INDEX	3
FINAL REPORT	4
I. Introduction	4
II. Correlation between fabrication parameters, index profiles, proton profiles and rocking curves.	4
II. 1. Fabrication of Proton exchanged waveguides	4
II.1.1. Reproducibility	4
II.1.2. Preparation and optical characterization of the first set of sample	5
II.1.3. Influence of the water	5
II.2. Rocking curves	18
II.2.1. Identification of the phases.	18
II.2.2. Water influence	18
II.3. SIMS analysis	34
III. Compatibility of PE process with the nonlinearity of the crystal	35
III.1. Influence of the Proton Exchanged process on the nonlinear coefficient	35
III.2. Influence of the Proton Exchanged process on the poling	39
IV. Conclusion	41
REFERENCES	42
APPENDIX 1 : SIMS MEASUREMENTS	43

Final report

I. Introduction

The study we proposed had the objective to establish correlations between the optical properties of the PE waveguides realized on LiNbO_3 and LiTaO_3 , their proton concentrations and their crystalline quality. Indeed these correlations are useful to determine the optimized fabrication conditions for each of the sophisticated devices combining sources and modulators on the same chip, that can be achieved using these substrates and this technology.

This work, which was planned over three years, has been divided into two parts. The first part, is to determine the correlation between fabrication parameters, index profiles, proton profiles and rocking curves. The second part will be to identify the influences of the protons, on the intrinsic properties of the crystals used or the properties of the dopant (rare earth) introduced in the crystals. With our collaborators, S.W. Novak at Evans East, Inc. NJ, USA and M. Laügt at CRHEA, Sophia-Antipolis, FRANCE we have realized and analyzed a first set of samples, covering a wide range of fabrication conditions. As the LiNbO_3 waveguides appeared to be more interesting for the applications, we have concentrate our efforts on this crystal for the first year. Using the phase diagram published by Yu. N. Korkishko¹, we have shown that the knowledge of the index profile and of one rocking curve measured on the 00.12 crystallographic plane using a High Resolution X-Rays Diffraction (HRXRD) equipment is necessary and sufficient to clearly identify the different crystallographic phases present in the exchanged layer. HRXRD spectra also show that all the phases are not obtained with the same quality, which explains the different losses observed in the waveguides. Index profiles and $[\text{H}^+]$ profiles show identical shapes (gradient or step like), but the extraordinary index increase is clearly not proportional to the proton concentration. As the SIMS results are available since a couple of weeks only, only the qualitative correlations are available know.

We have also started to study the different ways of producing waveguides in periodically poled material and the possibility of poling proton exchanged crystals. The preliminary results we have, show that there is a way to realize waveguides without domain erasure using a low acidity melt, and that a PE process involving a highly acidic melt could be used to pattern the domains.

The detailed report will be divided into two parts corresponding to the two main tasks that had been identify in this project :
correlation between fabrication parameters, index profiles, proton profiles and rocking curves
compatibility of the PE process with the nonlinearity of the crystal.

II. Correlation between fabrication parameters, index profiles, proton profiles and rocking curves.

II. 1. Fabrication of Proton exchanged waveguides

II.1.1. Reproducibility

As I mentioned in my second interim report, at the beginning of the contract we had to solve a severe reproducibility problem. On step index waveguides, we measured up to 10% fluctuations on the index increase of samples prepared with the same recipe. For the samples presenting graded index profiles with low δn_e , the situation was even worse : it was not always possible to avoid the formation of a surface layer presenting a high index increase and a step profile.

After a lot of investigation we identified two reasons for this lack of reproducibility. First, we demonstrate that these fluctuations were partially due to a non controlled amount of water incorporated in the benzoic acid - lithium benzoate mixture we use as a proton source. The second factor was more difficult to identify as it depends on the precision of the equipment we use rather than on the process parameters. Indeed, in order to insure a good homogeneity of the

melt, we had introduced a mixing procedure of the benzoic acid and the lithium benzoate powders. This homogeneity is obtained by shaking the powder mixture in a plastic bottle, which was used also to weight the two compounds. What we didn't know was that the electronic scale we used was terribly sensitive to electrostatic charges, charges which were much more important in the plastic bottle than in the glass tube we used before. This sensibility introduced big errors in the scale information. As the transition between step index waveguides (PE_I or PE_{II}) and pure graded index (PE_{III}) waveguides as a function of the lithium benzoate concentration in the benzoic acid melt is very sharp (Fig. 1), and as the amount of added lithium benzoate is very small ($\rho \leq 3\%$) this causes the process to be dramatically non reproducible.

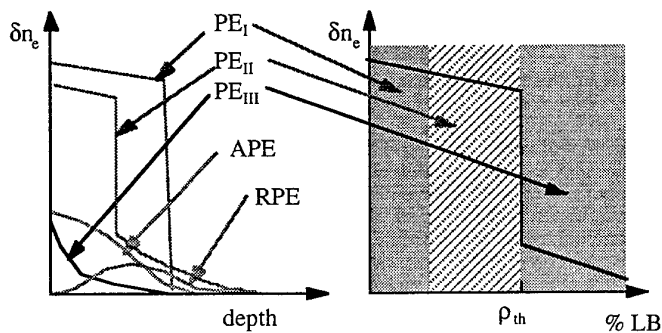


Fig. 1: Different kinds of index profile achievable by proton exchange.

APE is for annealed proton exchange

RPE is for reverse proton exchange

PE_I , PE_{II} , PE_{III} , are for the different kind of waveguides obtained by a single step exchange, varying the acidity of the melt. When the acidity is a function of the lithium benzoate amount in benzoic acid, the limit ρ_{th} between the PE_{II} and the PE_{III} region is very sharp and depends also on the temperature.

By drying the products with a lot of care and screening the electrostatics charges during the weighting process, we dramatically improved the control of the process and we have now a control of 1% on the extraordinary index increase.

II.1.2. Preparation and optical characterization of the first set of sample

Despite the reproducibility problem, we produce a first set of 10 samples whose fabrication parameters are listed in Table 1. These parameters have been chosen in order to obtain multimodes waveguides of all the kind achievable using benzoic acid melts. Using an He-Ne laser and a prism coupling set-up, we measured the effective indices of the different modes supported by the waveguides. Then, using the inverse WKB calculation² we deduced the index profiles that are given in fig. 2 to fig 9. Four of these waveguides show a step index profile with an extraordinary index increase of the order of 0.1. The six others present gradient index profiles with very different index variations varying from 0.1 to 0.01. The index profile of the samples prepared with more than 3% of lithium benzoate are not presented as they support only two modes which is not sufficient to reconstruct the index profile by this technique.

II.1.3. Influence of the water

As the influence of the water was more important in the case of PE_{III} waveguides, we have prepared 4 melts with a lithium benzoate content sufficient to produce PE_{III} waveguides and intentionally had some water (a few drops) to two of them before sealing the ampoule. The fabrication parameters of the corresponding samples are given in Table 2. The waveguides have then been characterized optically using the same set-up. Obviously the waveguides prepared with a wet mixture present a much higher index increase and a complex index profile which looks like a combination of a step region and a gradient region (Fig. 10 and Fig. 11).

Table 1 : Proton exchanged samples with dry melts

Sample	$\rho_{LB}(\%)$	$\Delta t_{exch} (h)$	$T_{exch} (^\circ C)$	350°C Annealing (h)	δn_e	Depth (μm)	Profile
NZ30-5B	4	15	300	0	0.008	2.5	gradient
NZ32-2	3.7	24	300	0	0.028	4.5	gradient
NZ30-11	1	6	300	6	0.045	5	gradient
NZ31-3	1	1	300	16,5	0.062	7	gradient
NZ30-2	1	1.5	300	1	0.100	5	gradient
NZ31-7	1	2.5	300	5	0.094	5	gradient
NZ31-16A	1	2.5	300	0	0.115	2	step
NZ30-3	1	2.5	300	0	0.114	2.9	step
NZ 32-1	0	1	300	0	0.111	3.2	step
NZ31-4	0	1	300	0	0.110	3	step

PROFILS DE G.O.P.

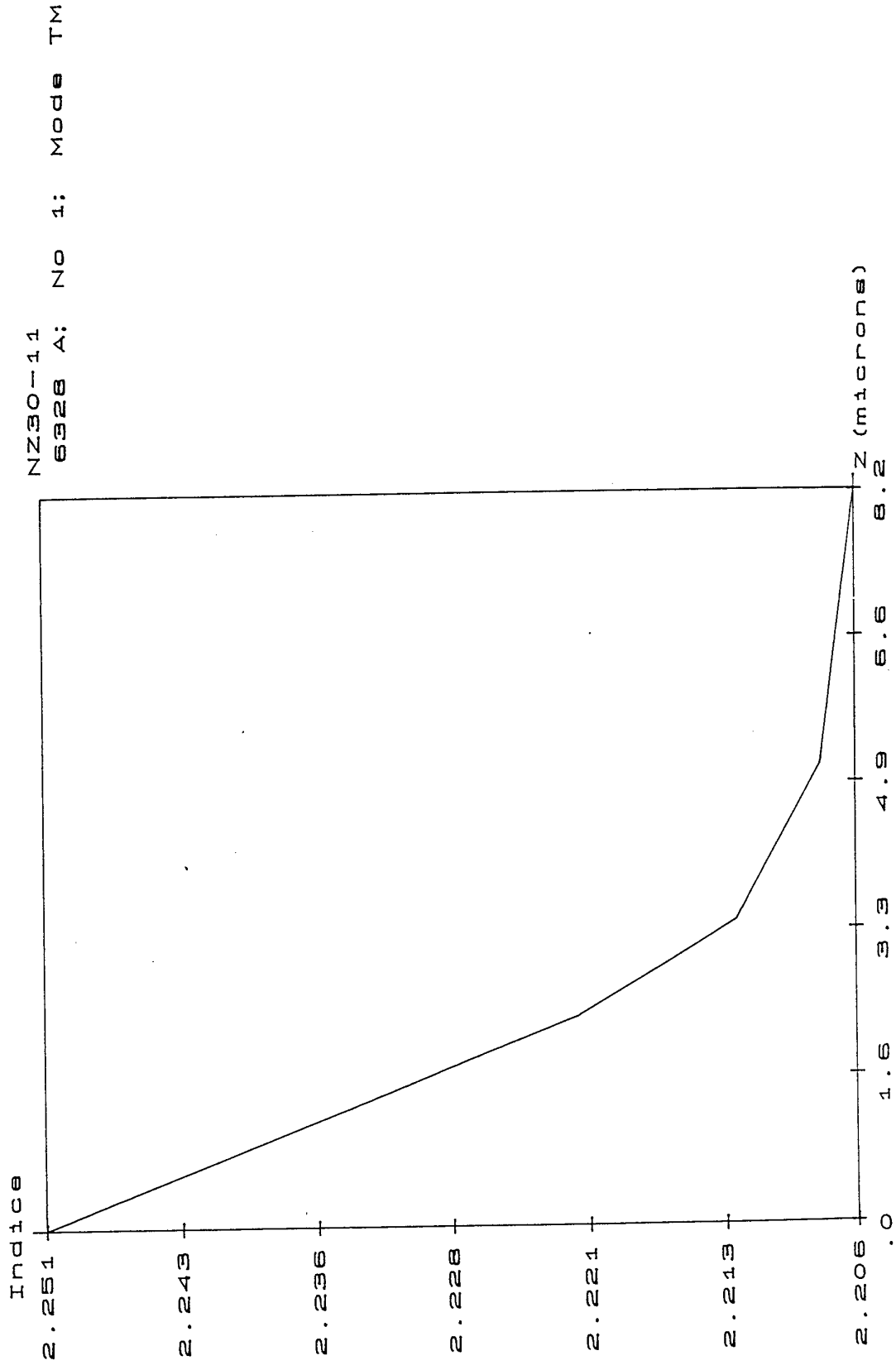


Fig. 2. Index profile of the sample NZ30-11

PROFILS DE G.O.P.

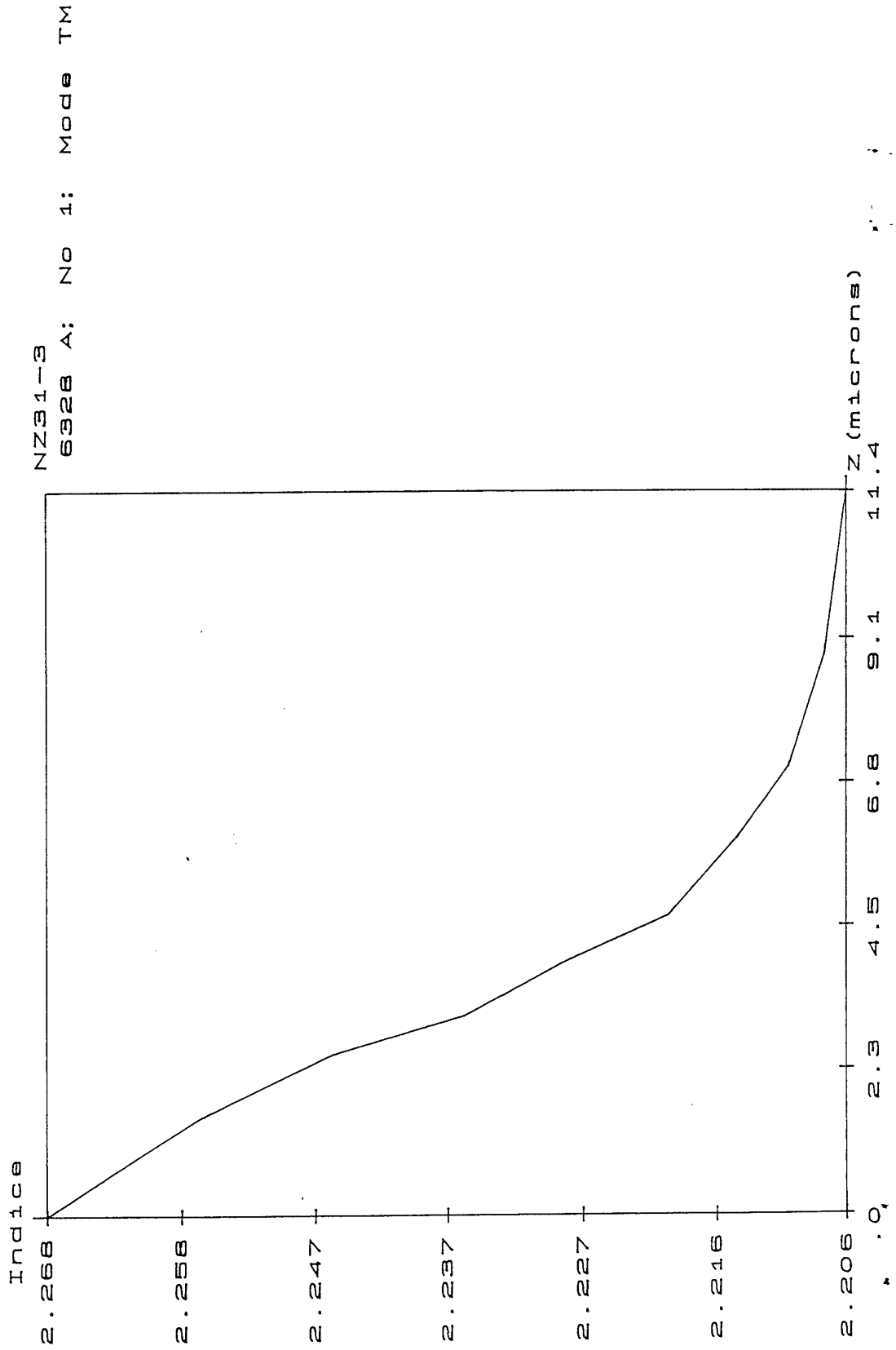


Fig. 3. Index profile of the sample NZ31-3

PROFILS DE G.O.P.

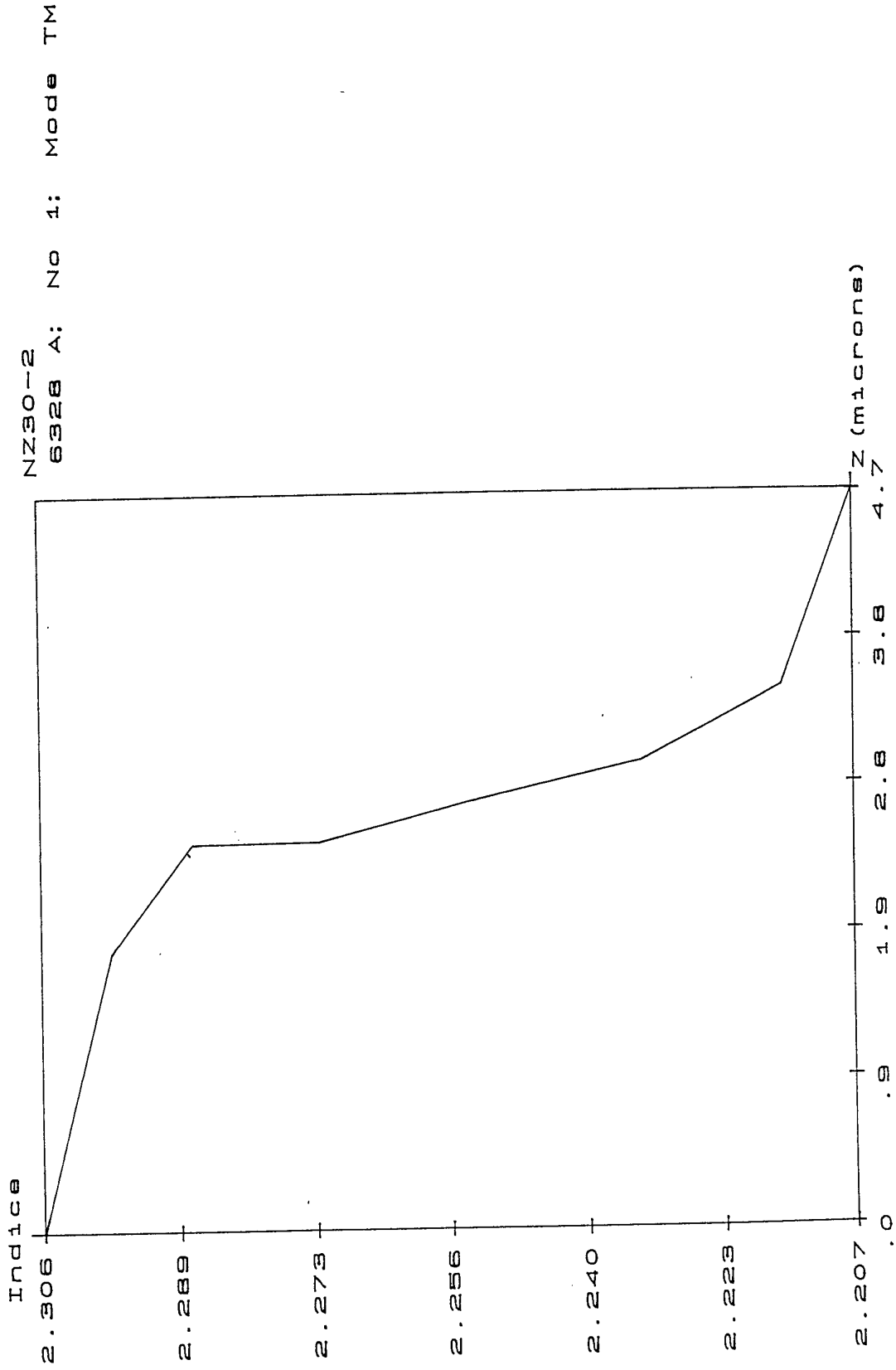


Fig. 4. Index profile of the sample NZ30-2

PROFILS DE G.O.P.

NZ31-7
6928 A: No 1: Mode TM

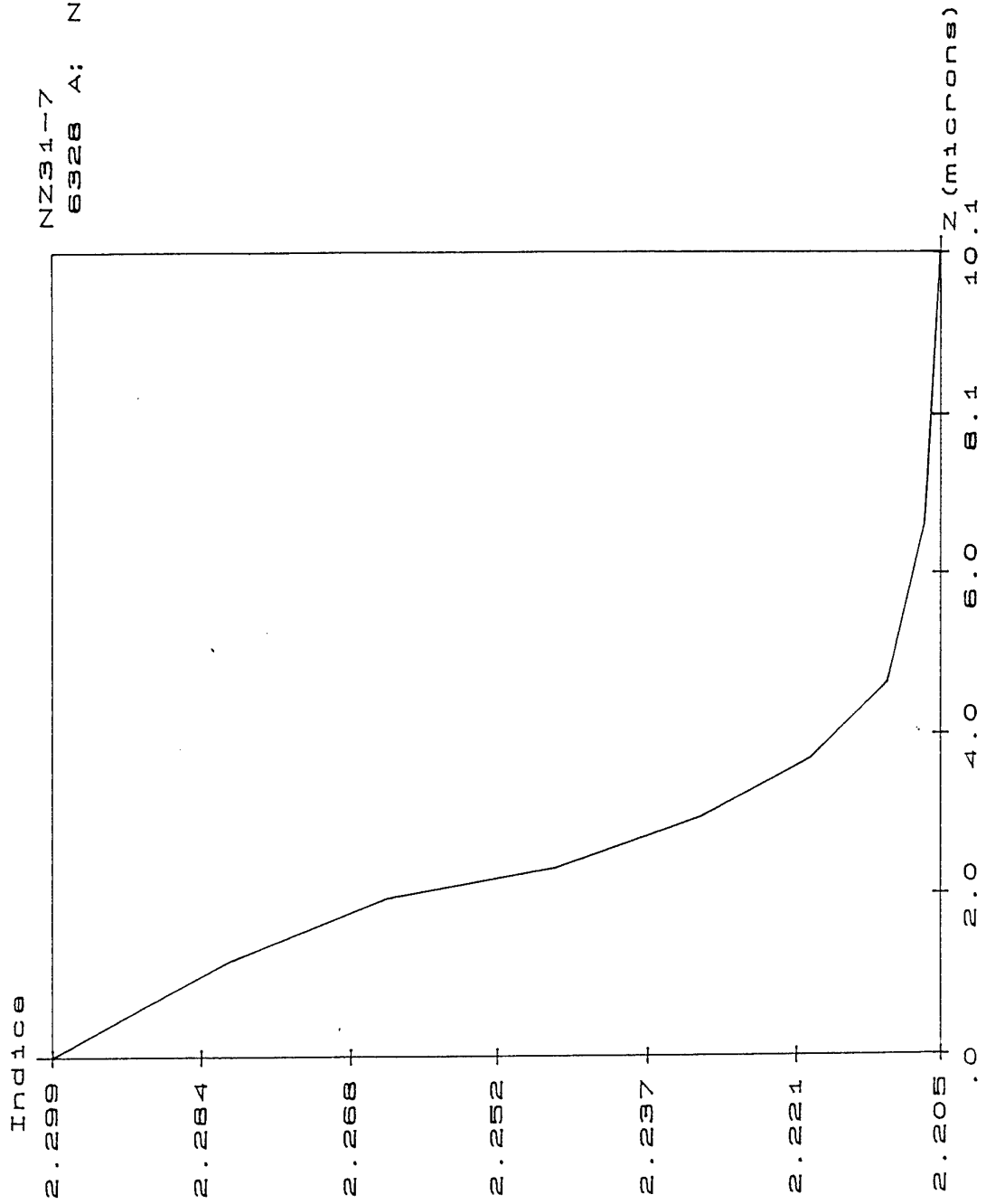


Fig. 5. Index profile of the sample NZ31-7

PROFILS DE G.O.P.

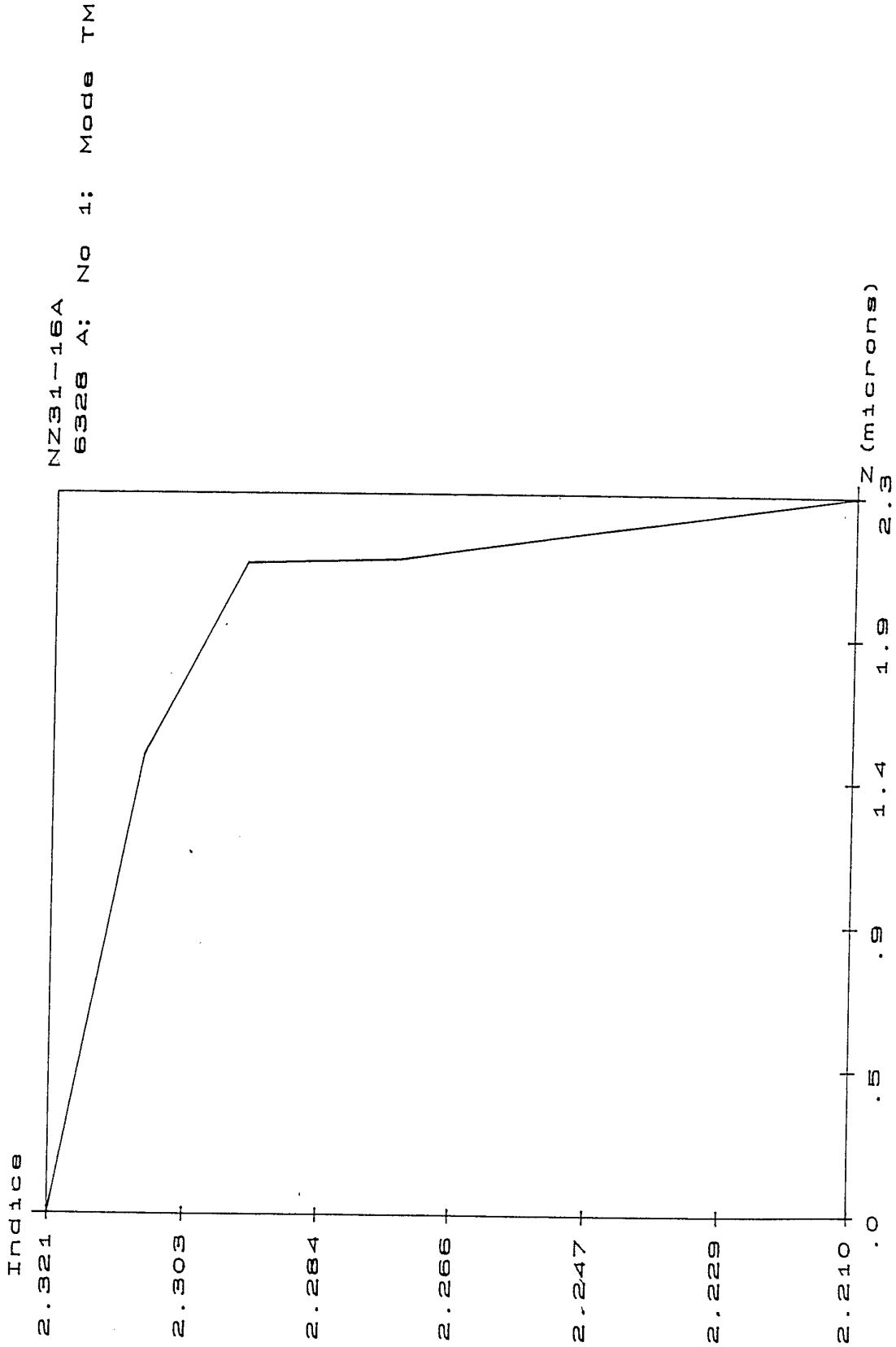


Fig. 6. Index profile of the sample NZ31-16A

PROFILS DE G.O.P.

NZ30-3
6328 A: No 1: Mode TM

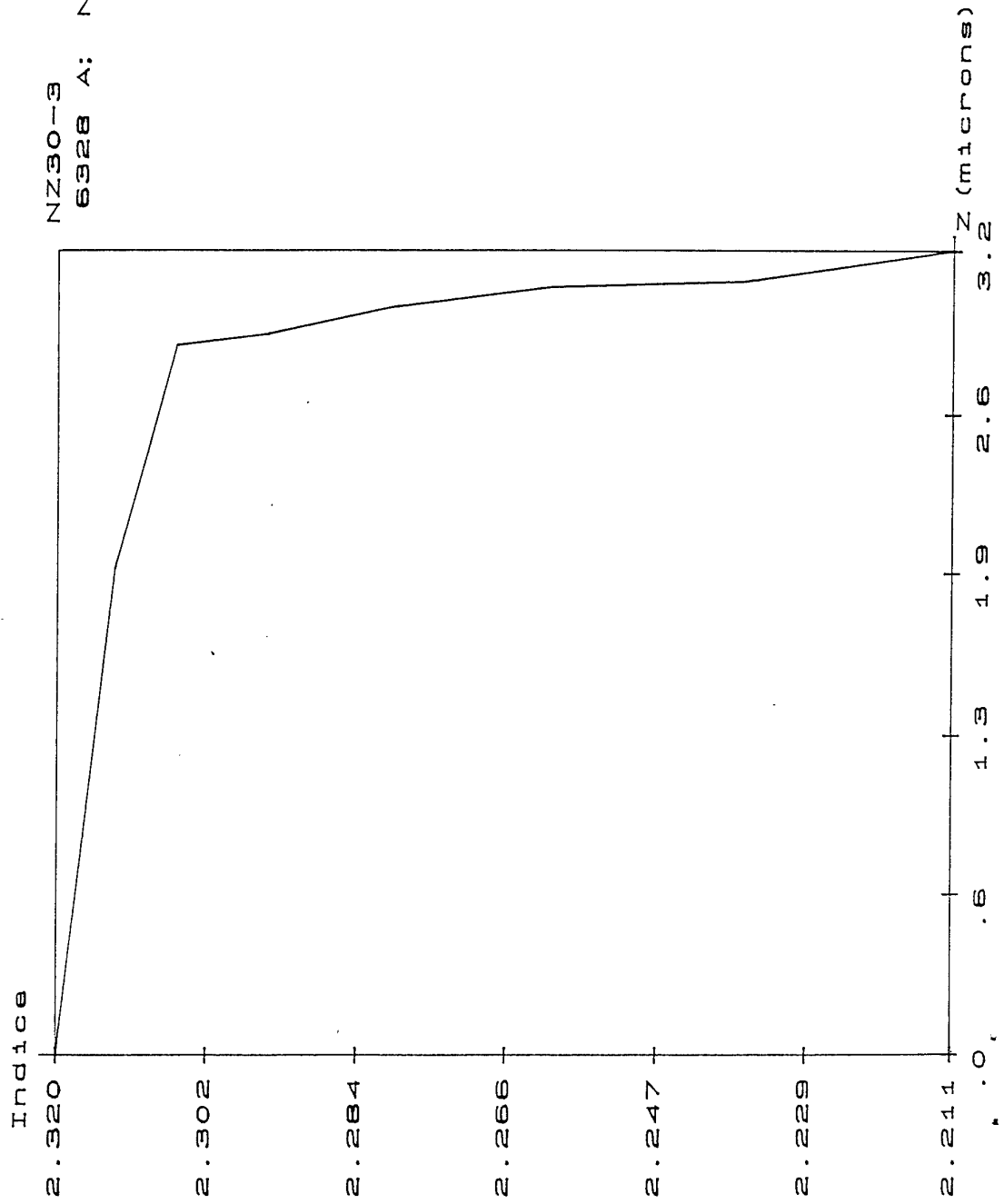
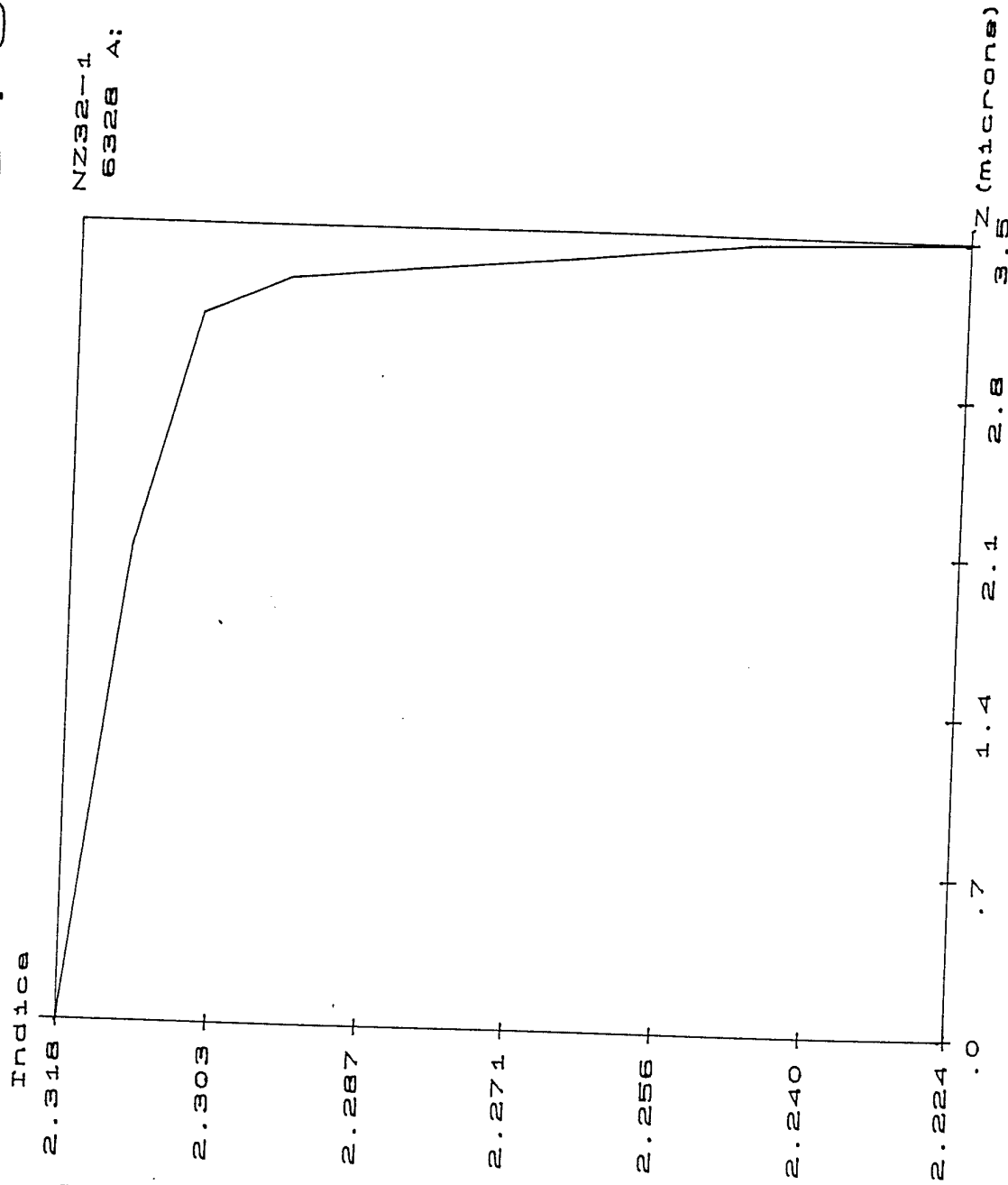


Fig. 7. Index profile of the sample NZ30-3

PROFILS DE G.O.P.

Influence of the proton concentration ...

NZ32-1
6328 A: No 1: Mode TM



8. Index profile of the sample NZ32-1

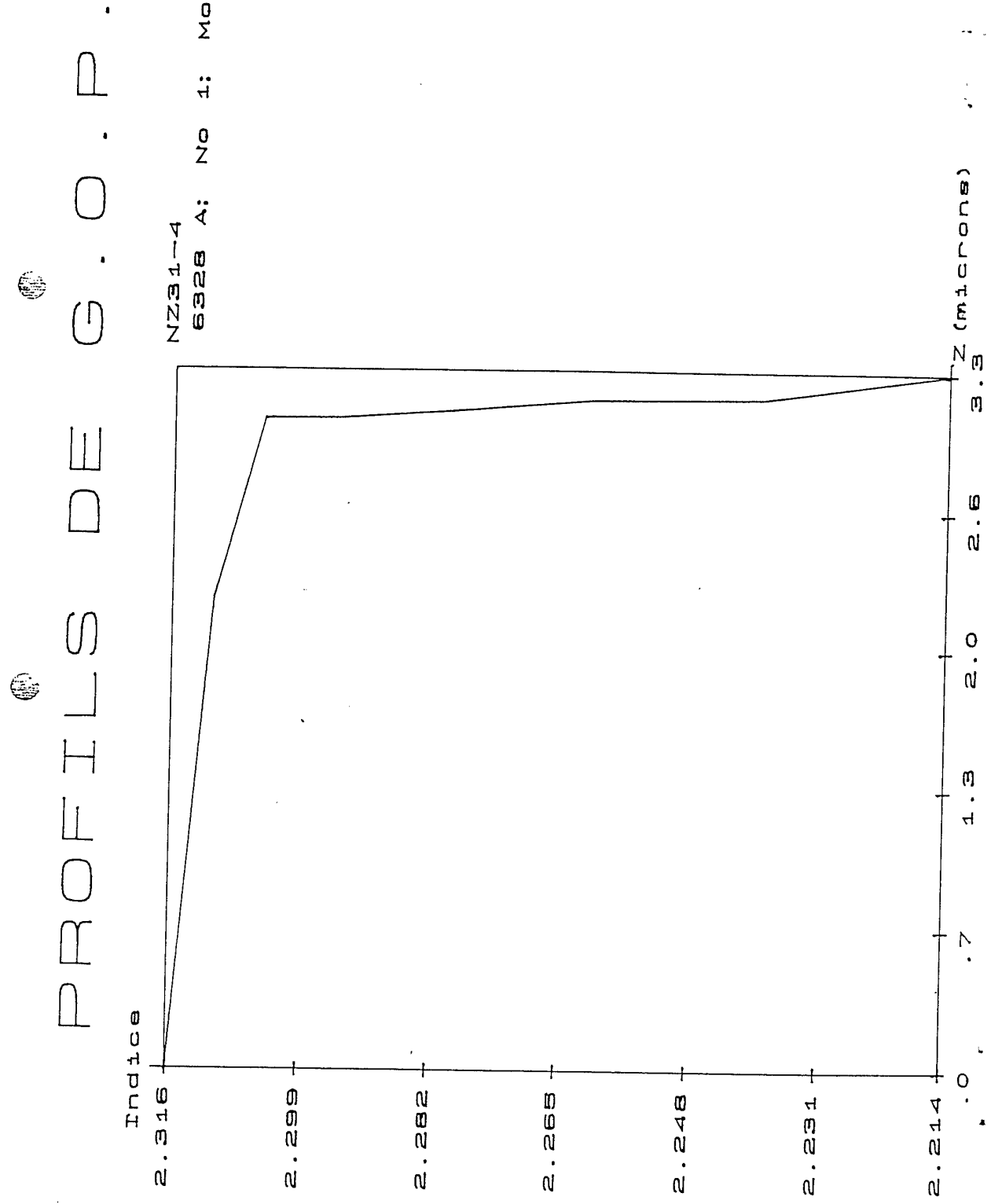


Fig. 9. Index profile of the sample NZ31-4

Table 2 : Exchange with low acidity melts and a varying quantity of water added before sealing the ampoule.

Sample	$\rho_{LB}(\%)$	$\Delta t_{exch} (h)$	$T_{exch} (^{\circ}C)$	350°C Annealing (h)	δn_e	Depth(μm)	Notes
NZ32-13B	2.5	24	300	0	0.070	1.5	water added
NZ33-13B	2.7	48	300	0	0.018	3	
NZ33-3B	2.7	24	300	0	0.019	2	
NZ33-13A	2.7	48	300	0	0.069	4	water added

PROFILS DE G.O.P.

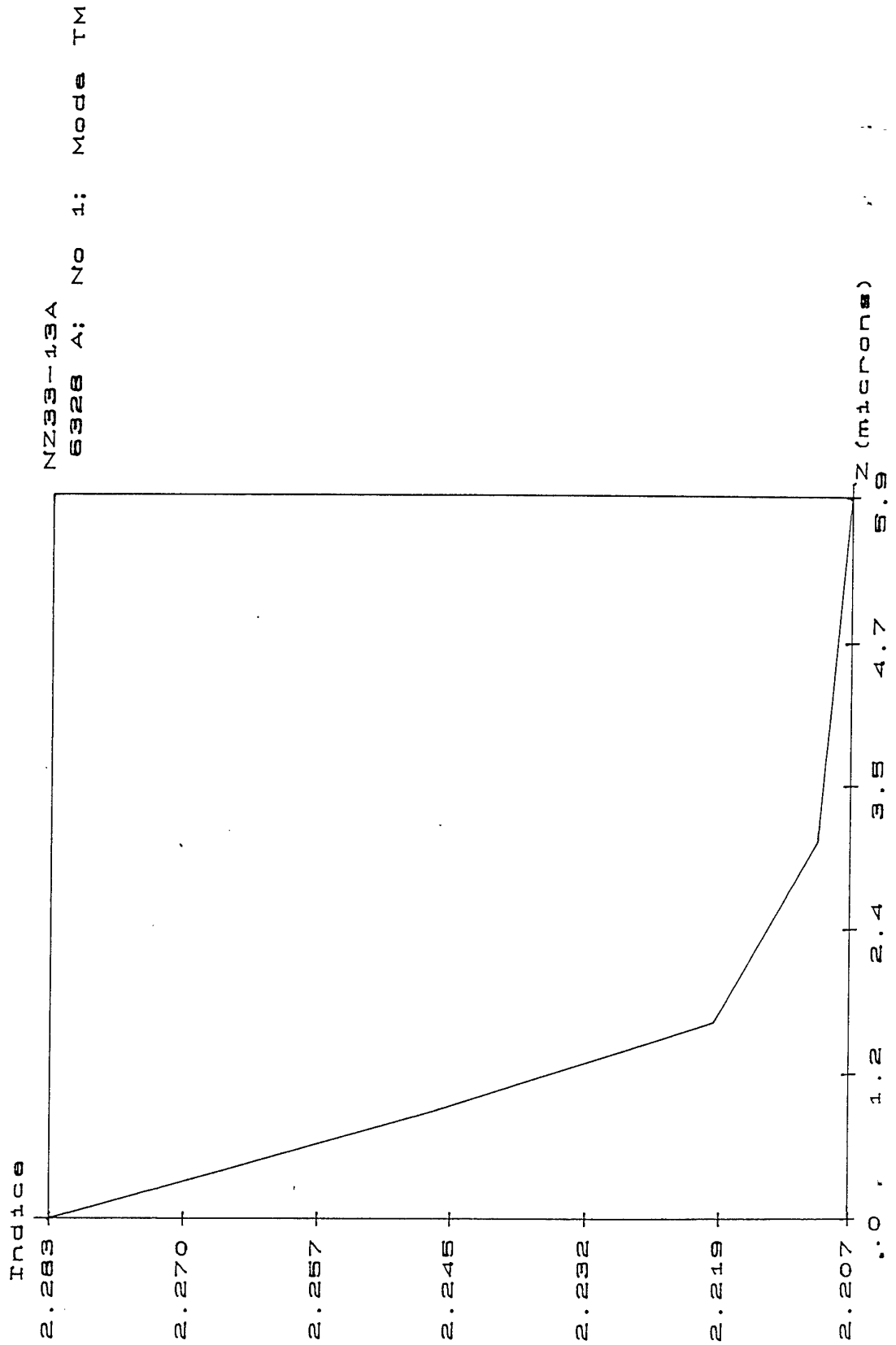


Fig. 10. Index profile of the sample NZ33-13A

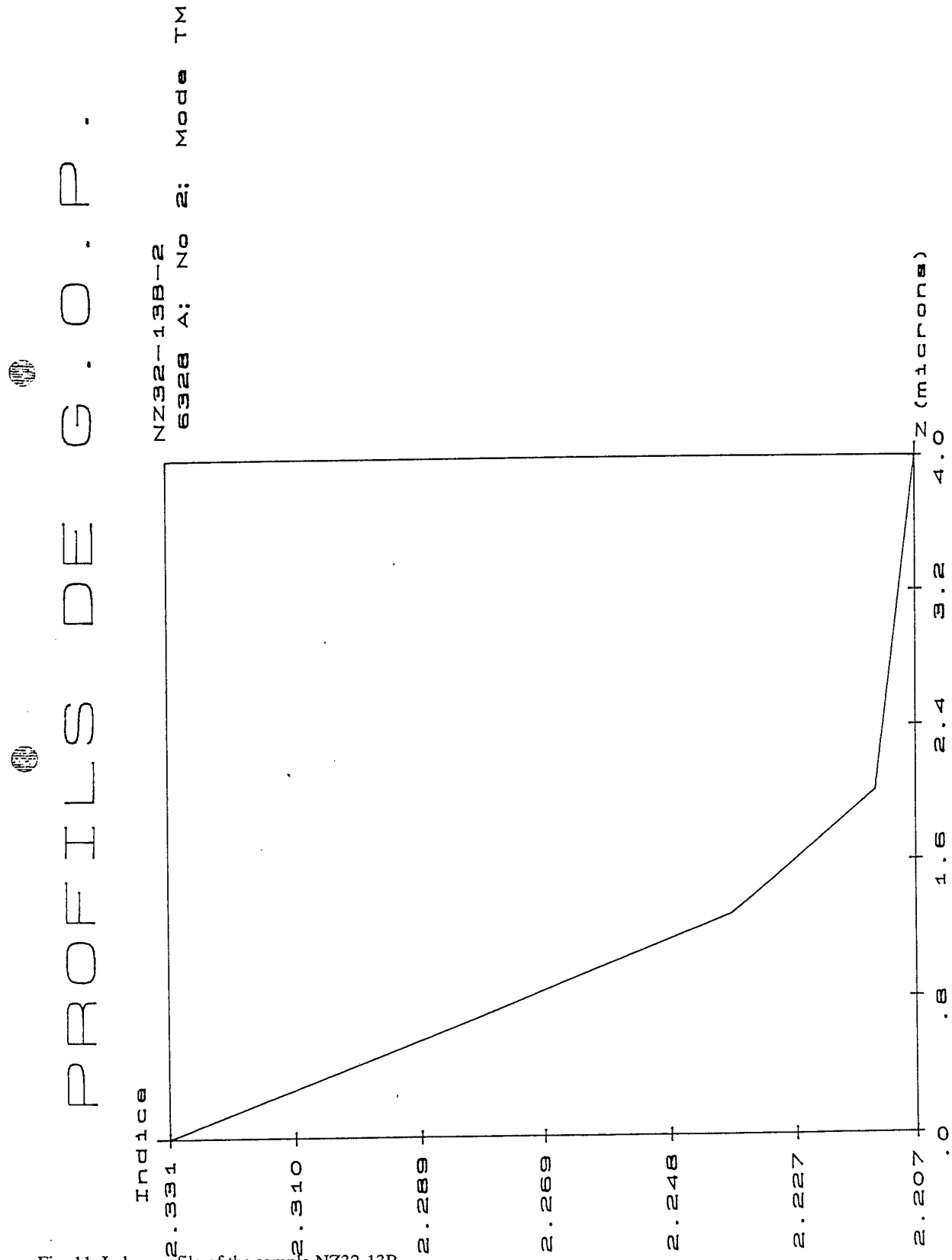


Fig. 11. Index profile of the sample NZ32-13B

II.2. Rocking curves

II.2.1. Identification of the phases.

On all these samples, rocking curves have been performed using a High Resolution X-Rays Diffraction (HRXRD) equipment. The curves obtained using the (00.12) crystallographic plane are reported in fig. 12 to fig. 21. Their correlation with the index profiles and the use of the phase diagram (Fig. 22) we established for Z-cut substrates indicate that we have succeeded in preparing two waveguides of each phase accessible using benzoic acid melts : α , β_1 , β_2 , κ_1 and κ_2 .

PE_{III} waveguides present a very small modification of the cell parameters (α phase) which correlates very well with the very high quality of the waveguides prepared using this recipe. Comparing the other spectra, shows that the β_1 layers have a better crystalline quality as the peak corresponding to the exchanged layer is very thin, signature of a very well organized layer. Careful loss measurements will be performed to compare the optical quality of the β_1 and the β_2 waveguides which present very similar index profiles.

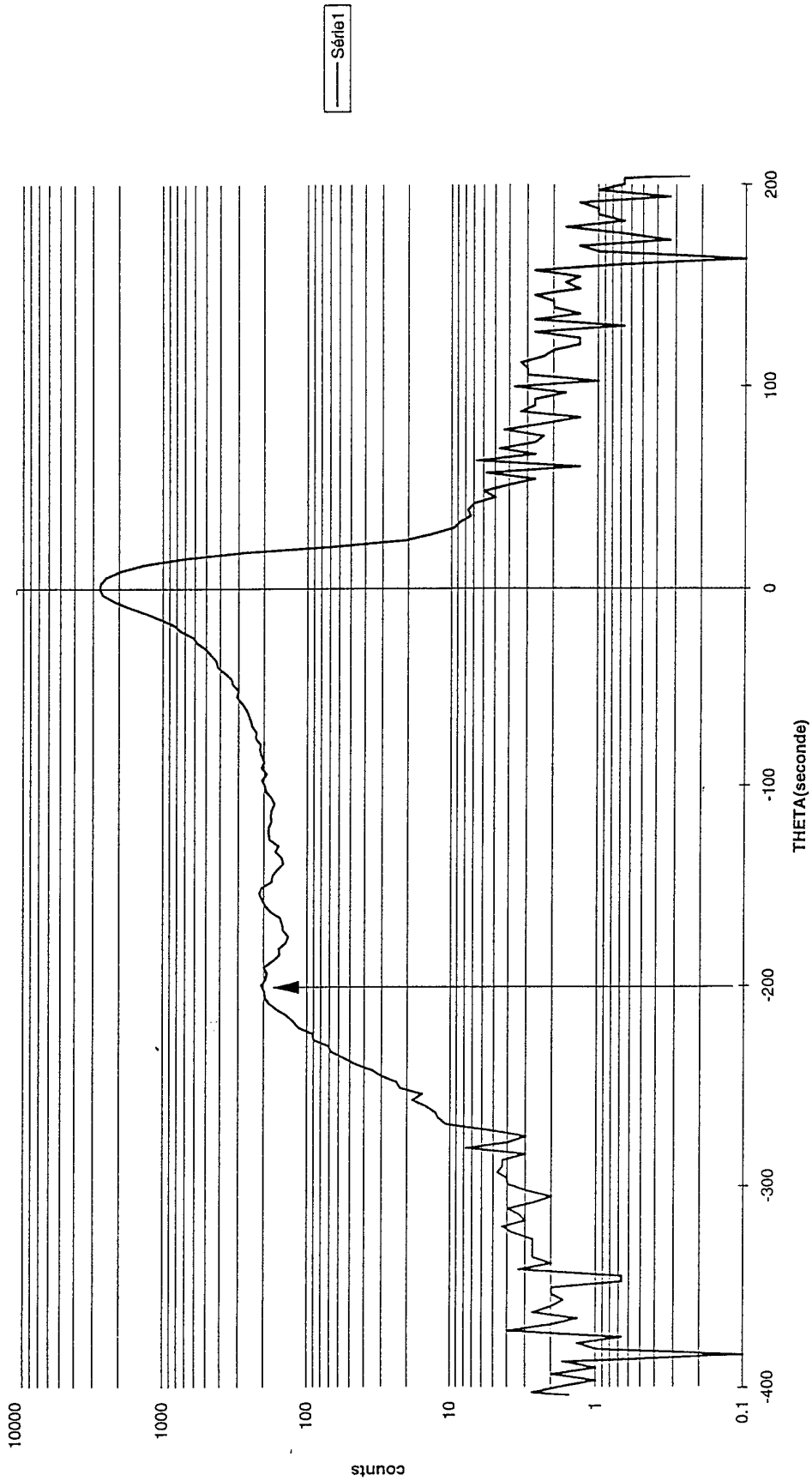
Comparing the samples of the same phase when they present different index increase, show a good correlation between the index increase and the strain : the higher the index the greater the strain. In β_2 phase, we expect the reverse correlation, but we cannot verify it, as the two samples of this first set present exactly the same index.

II.2.2. Water influence

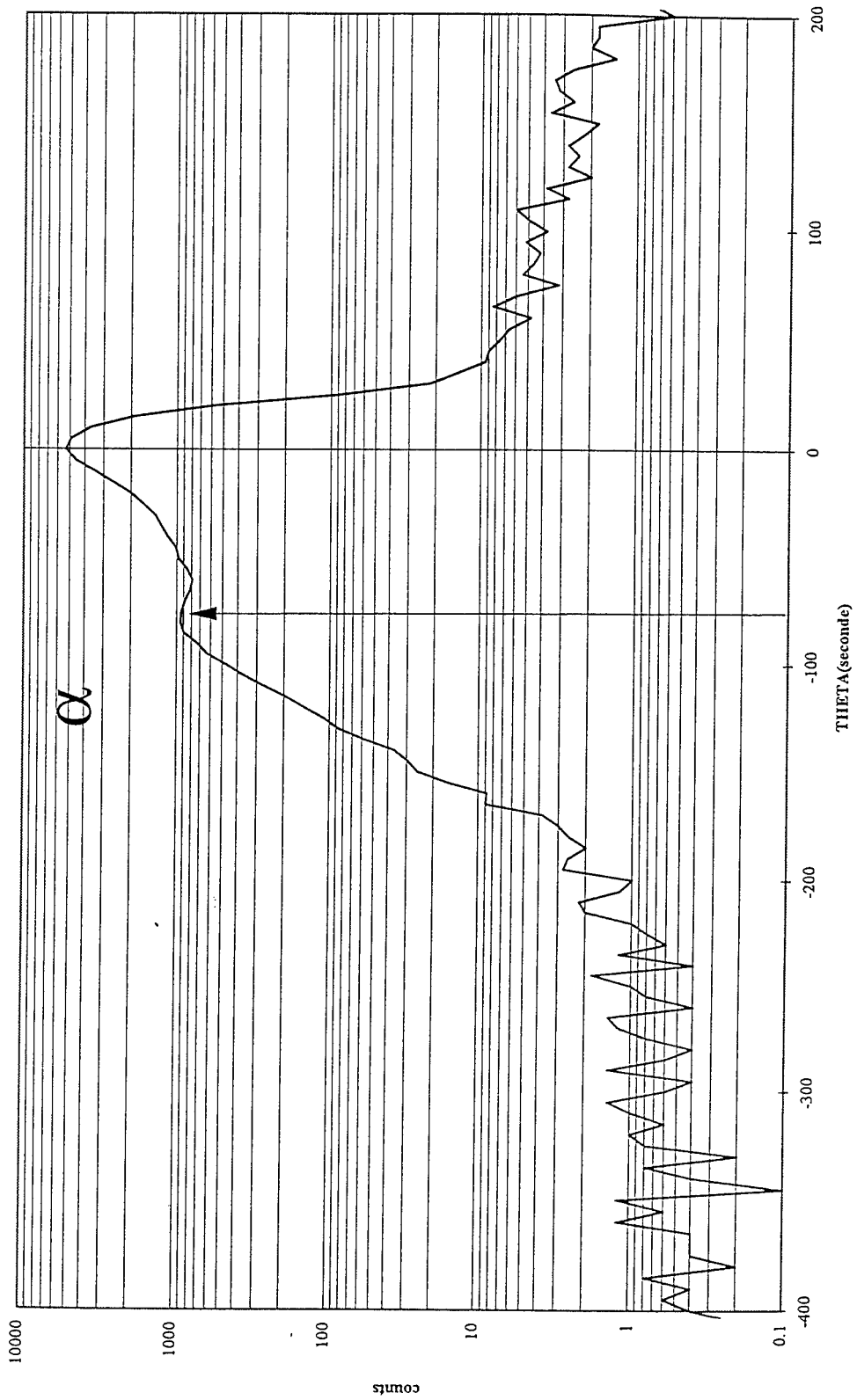
The set of samples prepared with a low acidic melt, but with varying amount of water, shows that the presence of water completely modifies the exchange process. Indeed the HRXRD spectra show that sample prepared with « wet » melts presents κ layers (fig. 23 to fig. 27) associated with a higher index increase. We suspect that the presence of water modifies dramatically the equilibrium between the H^+ and the Li^+ ions in the melt, which explains that the minimum amount of lithium benzoate, necessary to prevent the formation of the high index layers, is completely changed.

This study has also shown that the quality of the waveguides prepared with « wet » melts is lower than that of those prepared without added water. So, despite the fact that adding a measurable amount of water to the melt was a good and easy way to control its humidity, we decided to dry the melt by heating it during the evacuation of the ampoule. This process is somehow more difficult to control and we are working on the practical set-up allowing to dry the powder without taking a chance to evaporated part of the benzoic acid which then modifies the ratio between the acid and its lithium salt.

DDX sur NZ30-5B (0.0.12)

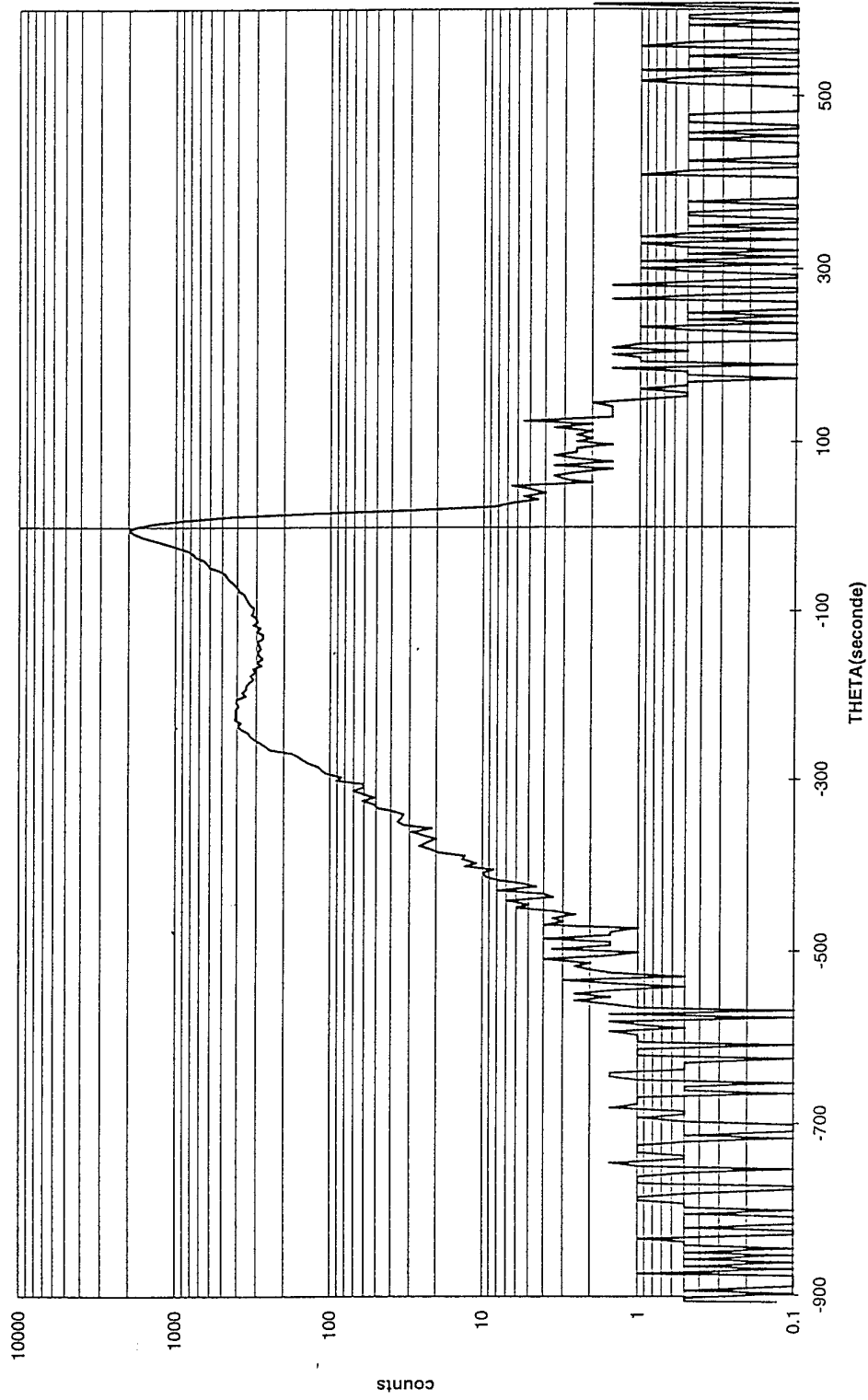


DDX sur NZ32-2 (0.0.12)



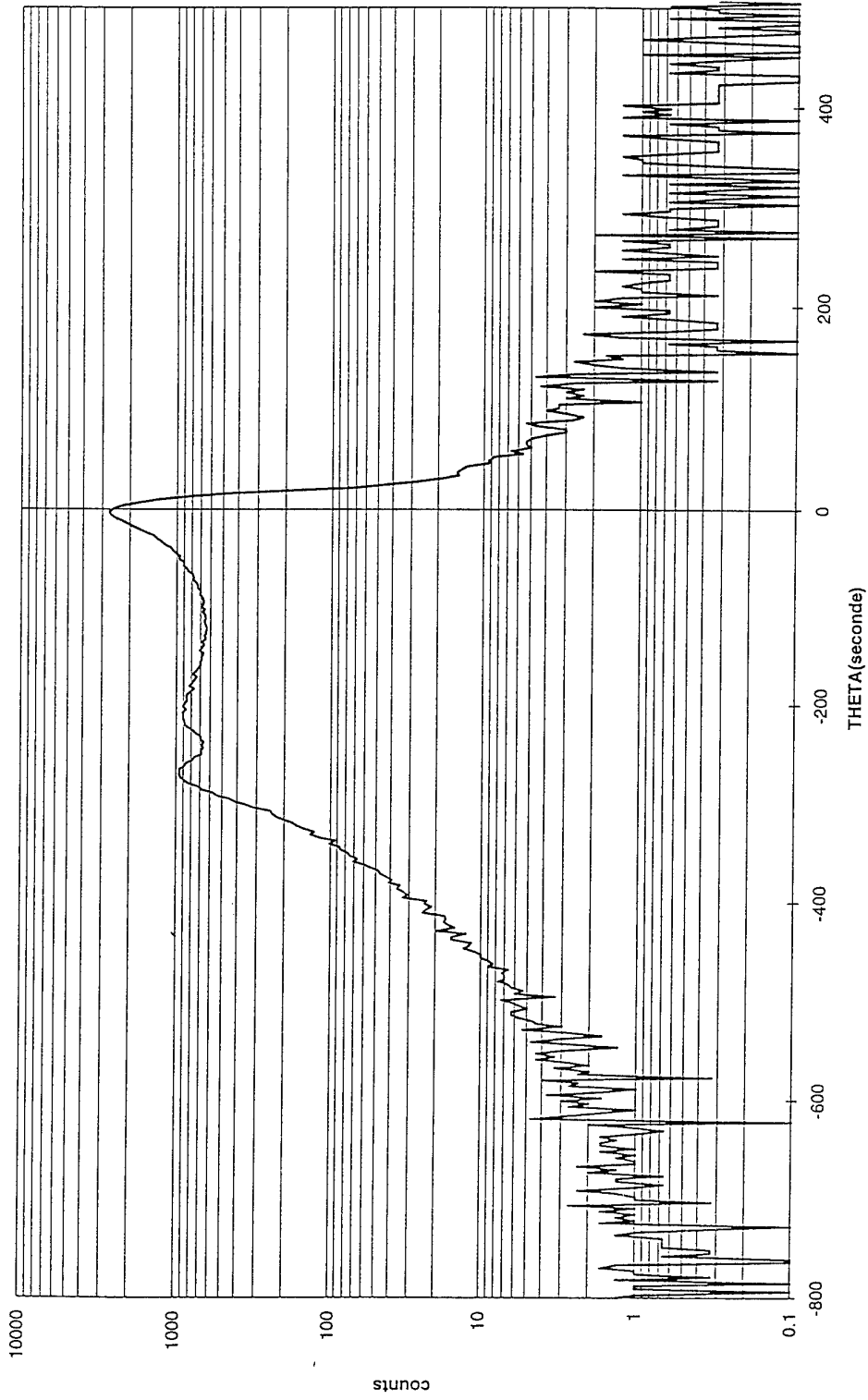
— Série

DDX sur NZ30-11 (0.0.12)

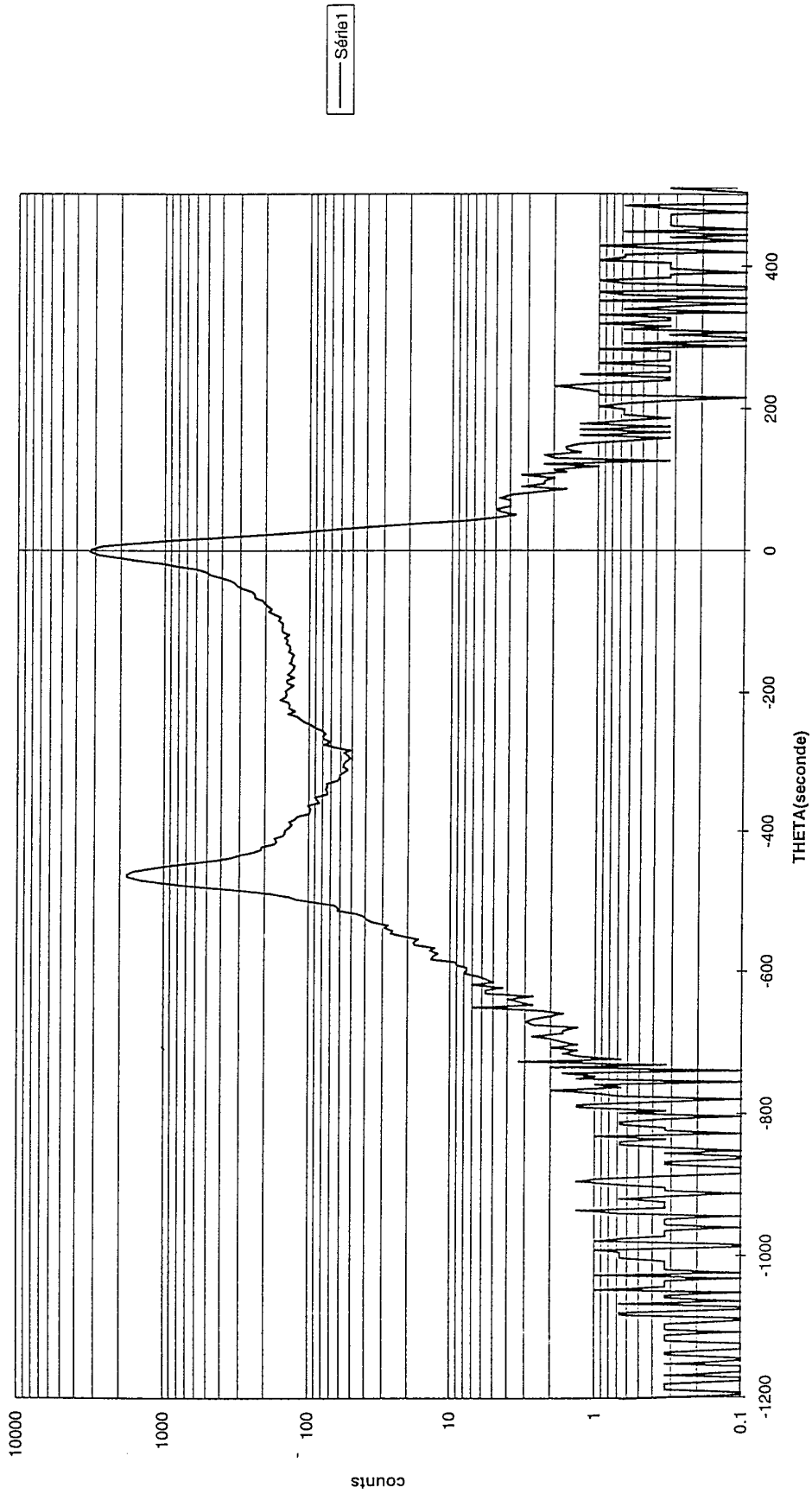


— Série 1

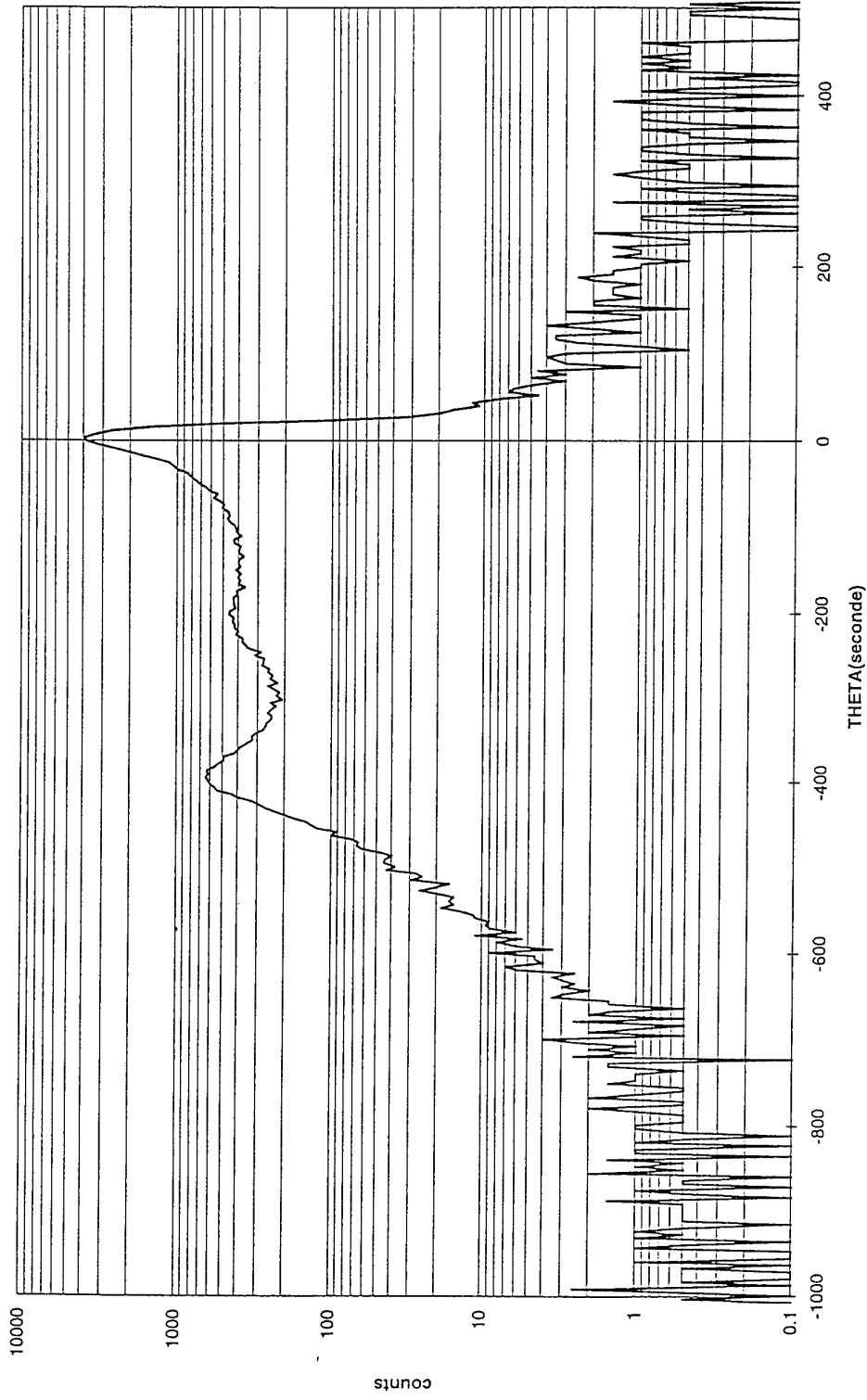
DDX sur NZ31-3 (0.0.12)



DDX sur NZ30-2 (0.0.12)



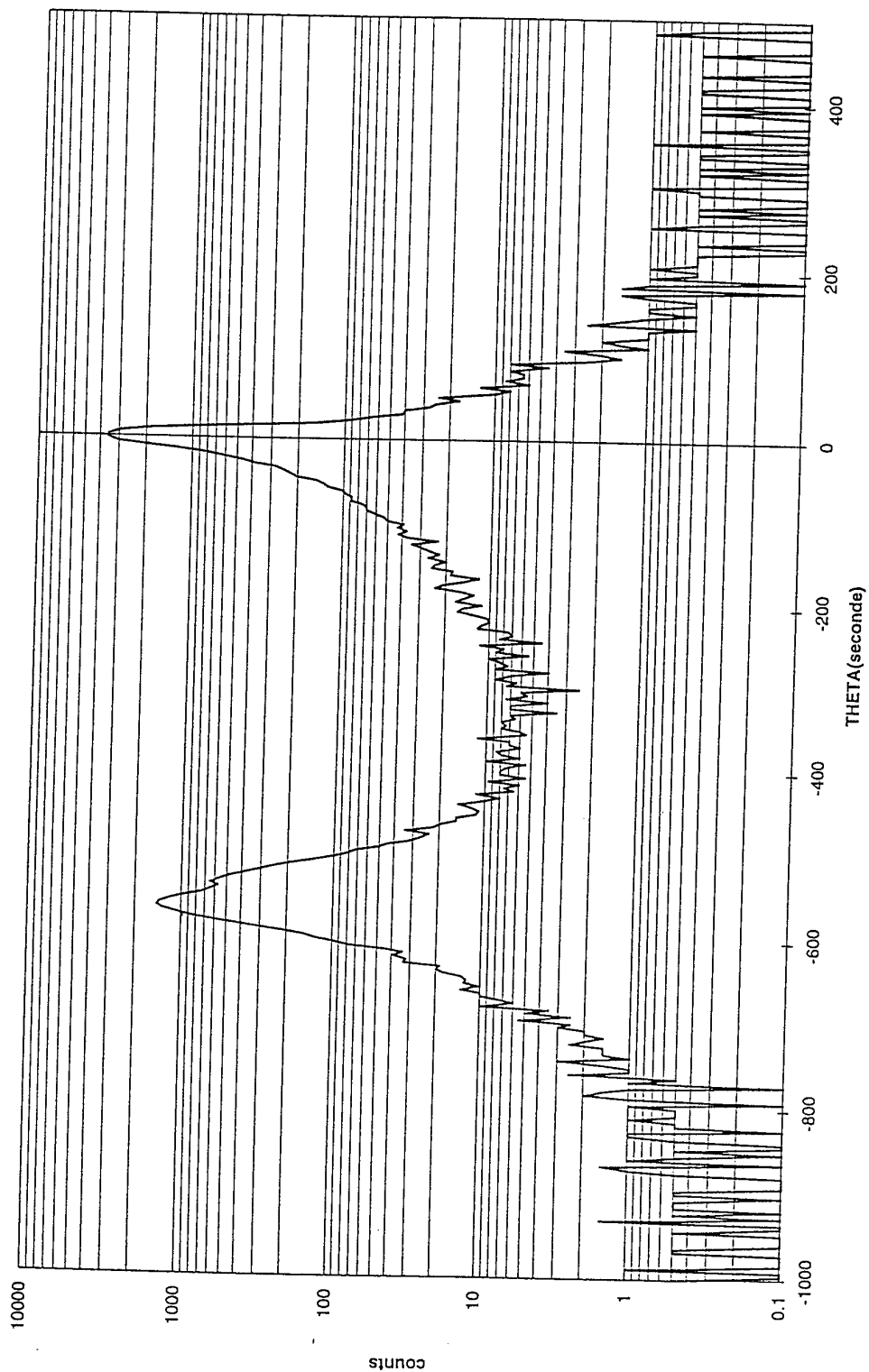
DDX sur NZ31-7 (0.0.12)



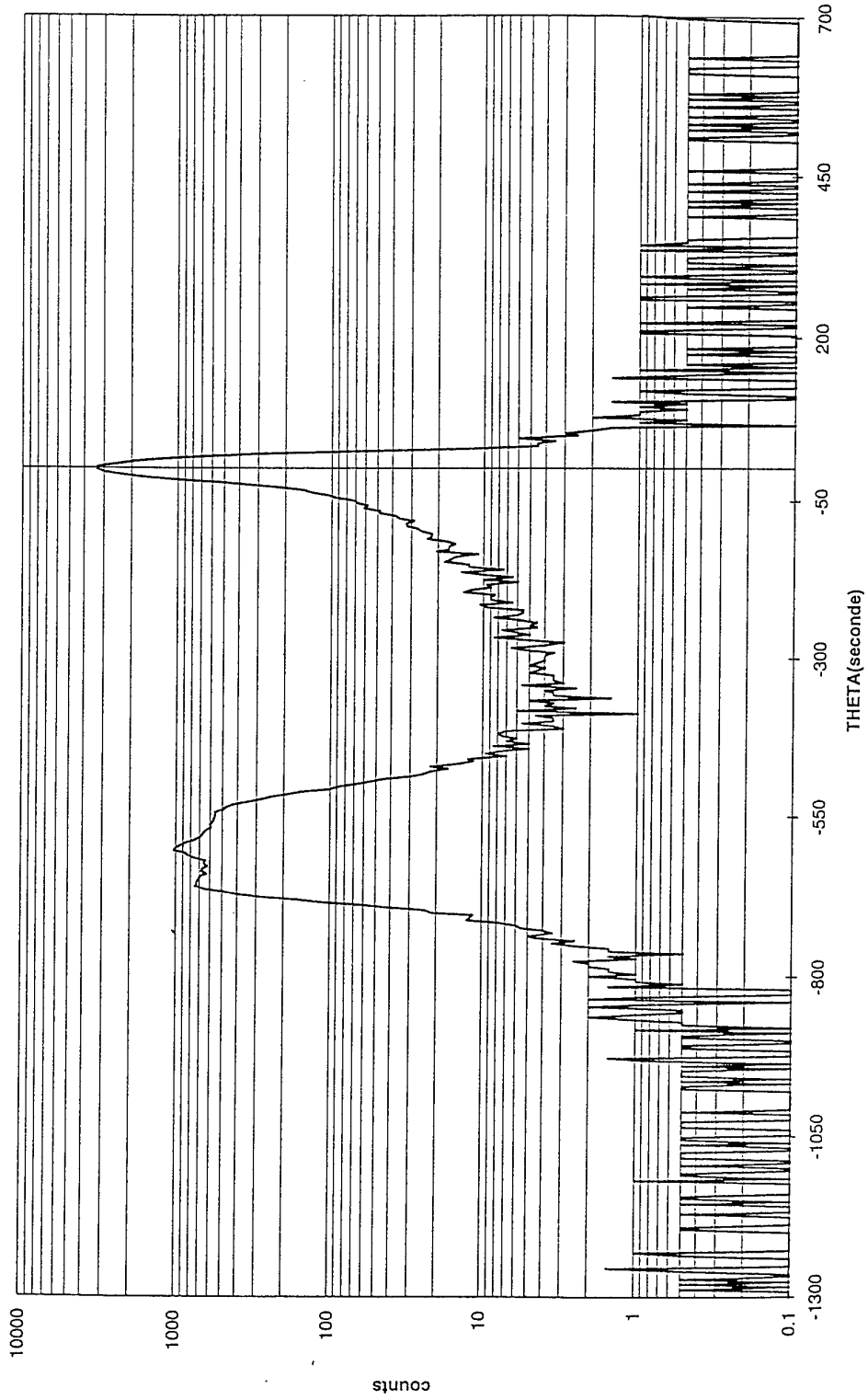
Série 1

— Série1

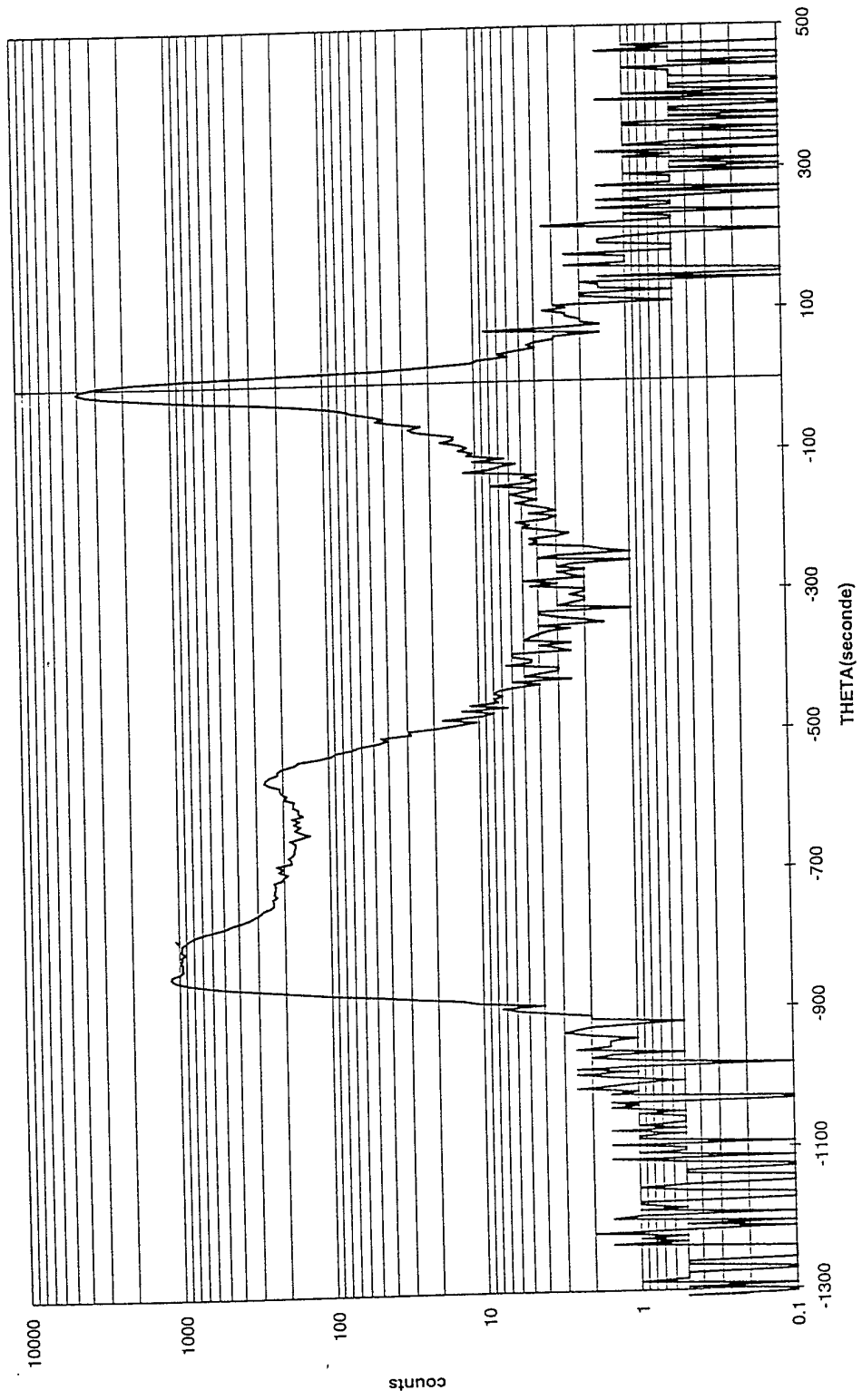
DDX NZ31-16A sur (0.0.12)



DDX NZ30-3 sur (0.0.12)

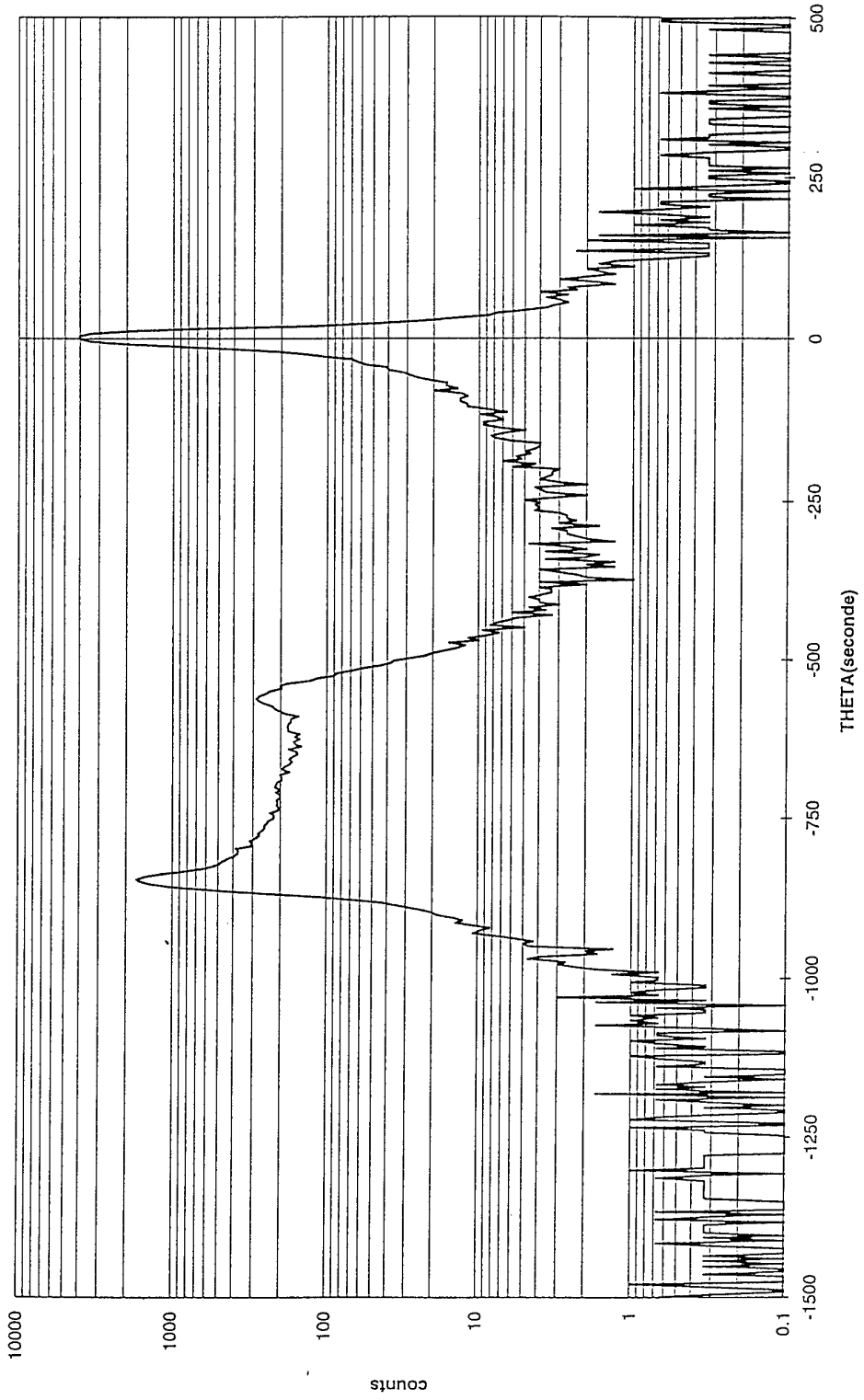


DDX sur NZ32-1 (0.0.12)



— Série 1

DDX NZ31-4 sur (0.0.12)



Série1

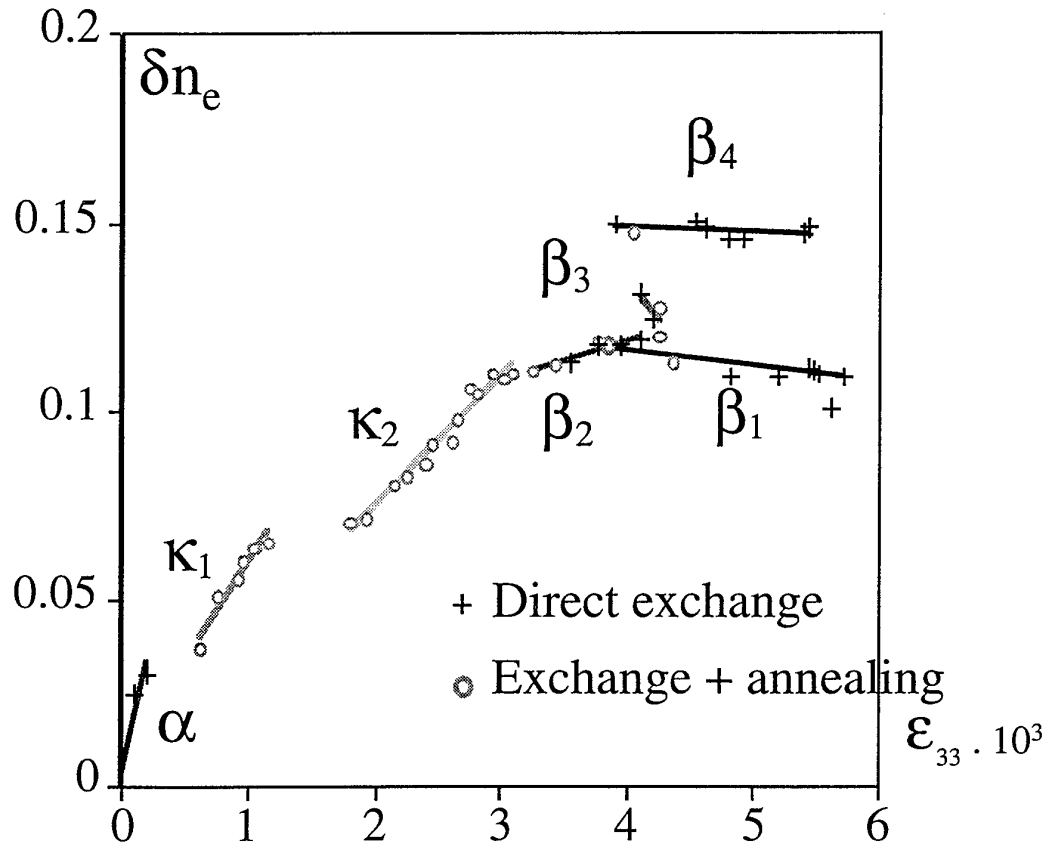
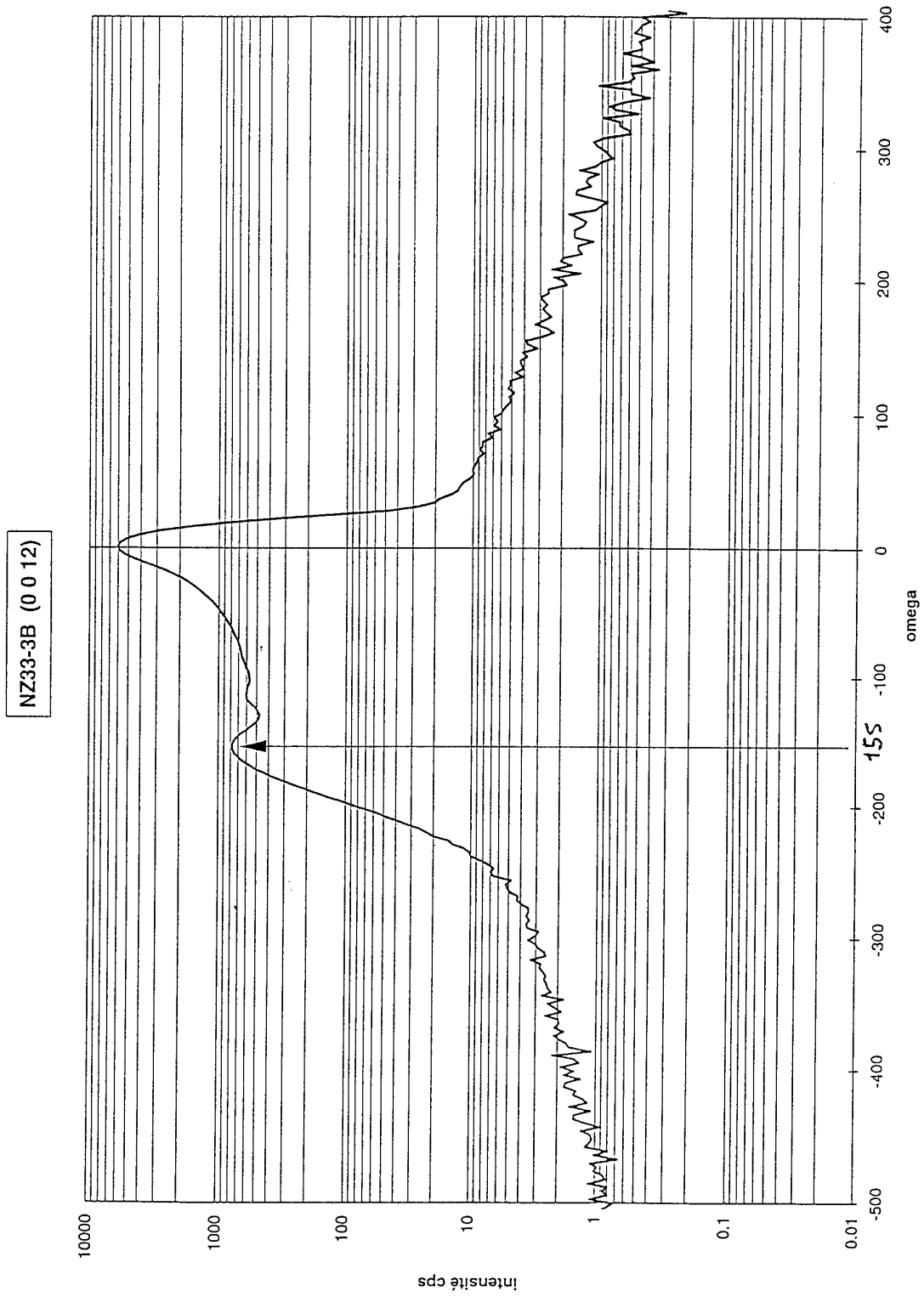
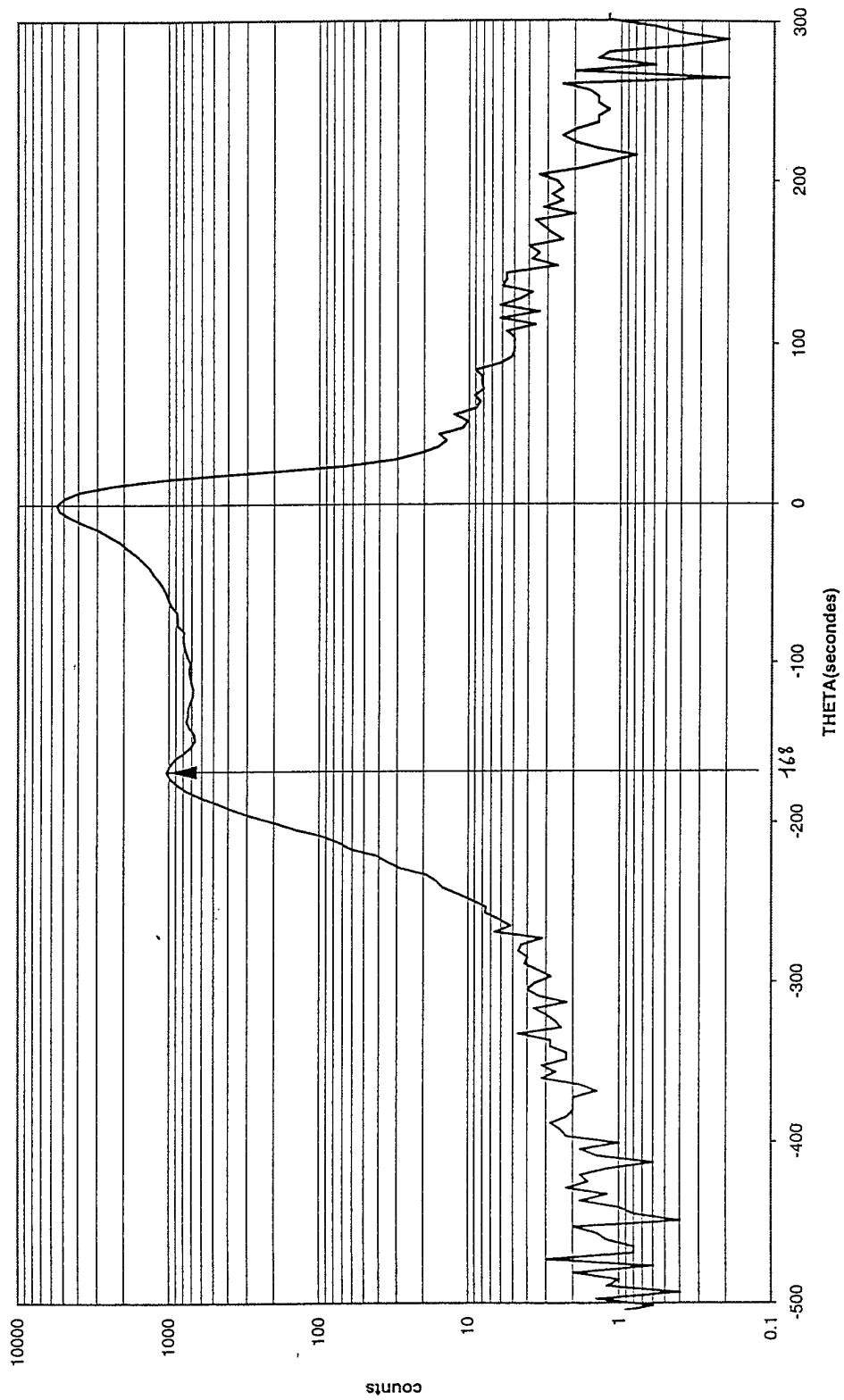


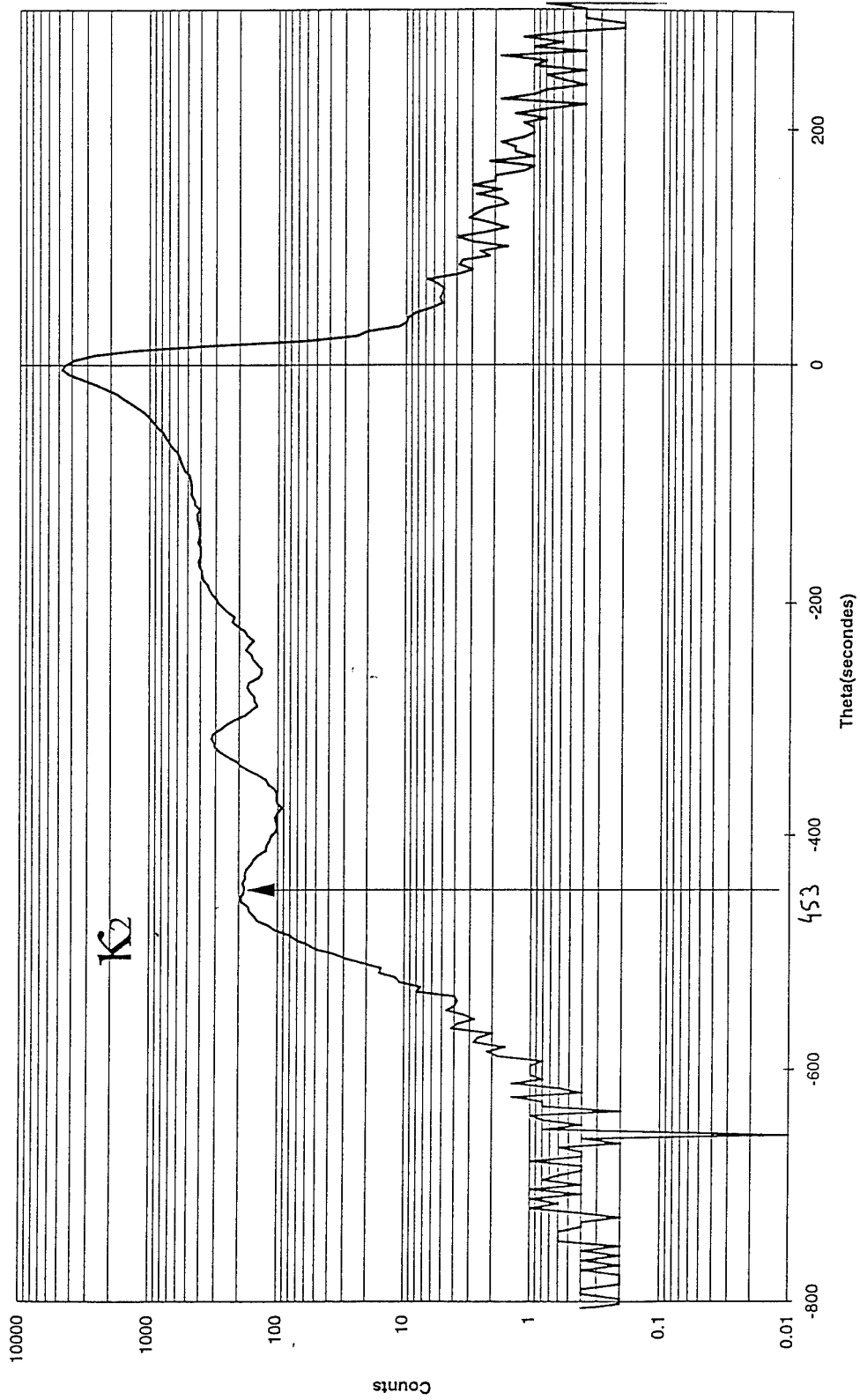
Fig. 12. Phase diagram of the PE layers on Z-cut substrates. The index increase is presented versus the relative strain induced in the PE layer along the optical axis.



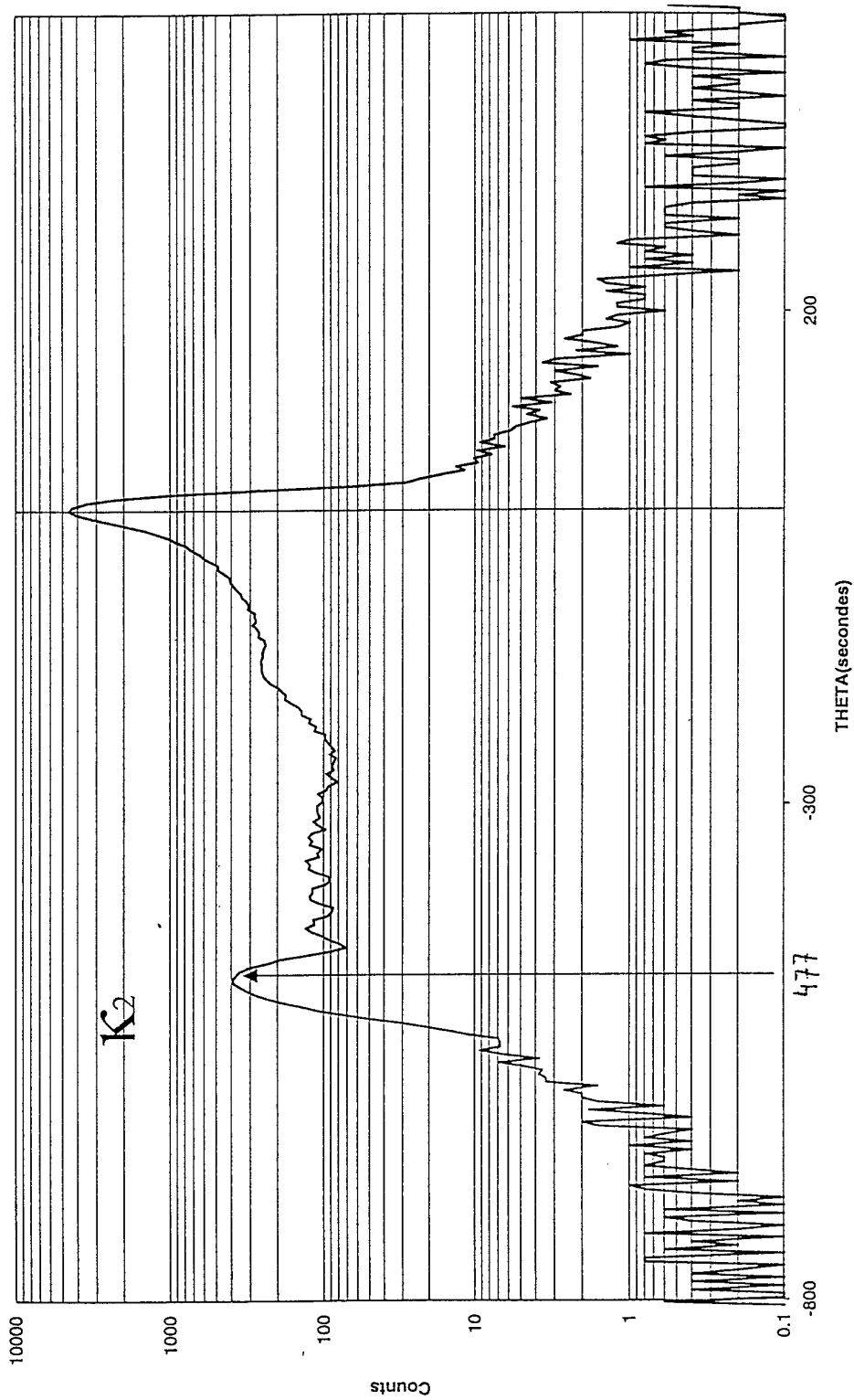
NZ33-13B(0.0.12)



DDX NZ33-13A(0.0.12)



NZ32-13B(0.0.12)



II.3. SIMS analysis

SIMS analysis has been performed on these samples (see report in Appendix 1). The first observation show straight forward correlation between step and graded index and H profiles. Taking into account the precision of the different processes, the depth obtained by optical characterization ($\pm 0.2 \mu\text{m}$) and by SIMS are identical.

Comparing the surface index increase and the maximum of the proton concentration, indicates a more complicated behavior. As expected from our previous experience the relationship between the index increase and the proton concentration is far from linear (Fig. 28). This is not contradictory with what has been observed previously on heavily annealed samples³, but underline the importance of the fabrication condition and the necessity to proceed to all the measurements (index profiles, rocking curves and $[\text{H}^+]$ profiles) on the same samples in order to be able to establish correlations. This plot also tends to indicate that the result obtained on sample NZ30-5B is somehow erroneous, but further investigations have to be done to produce quantitative conclusions.

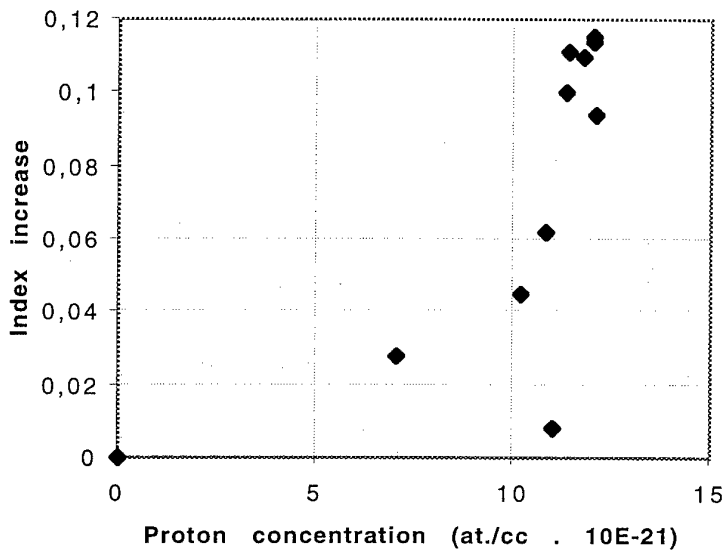


Fig. 28. Surface refractive index increase at $\lambda=632,8 \text{ nm}$ as a function of the maximum proton concentration measured by SIMS. The result obtained with sample NZ30-5B ($\delta n_s=0.008$) seems to be erroneous.

III. Compatibility of PE process with the nonlinearity of the crystal

III.1. Influence of the Proton Exchanged process on the nonlinear coefficient

Despite the reproducibility problems, some preliminary experiment aiming at measuring the nonlinear coefficient of different exchanged layers have been performed. They have shown dramatic differences depending on the recipe.

The experimental set-up is designed in order to measure the reflected SHG signal when an intense pump beam at $1.06 \mu\text{m}$ is focused on the polished edge of the waveguide. Fig. 29.

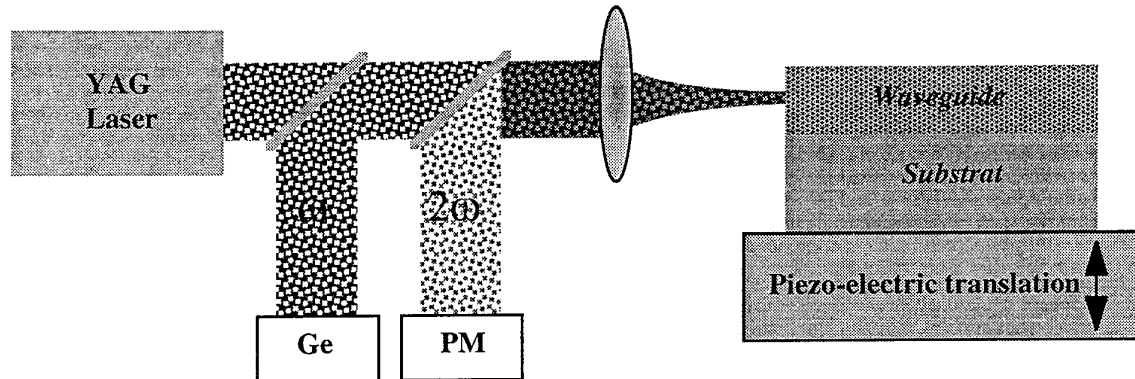
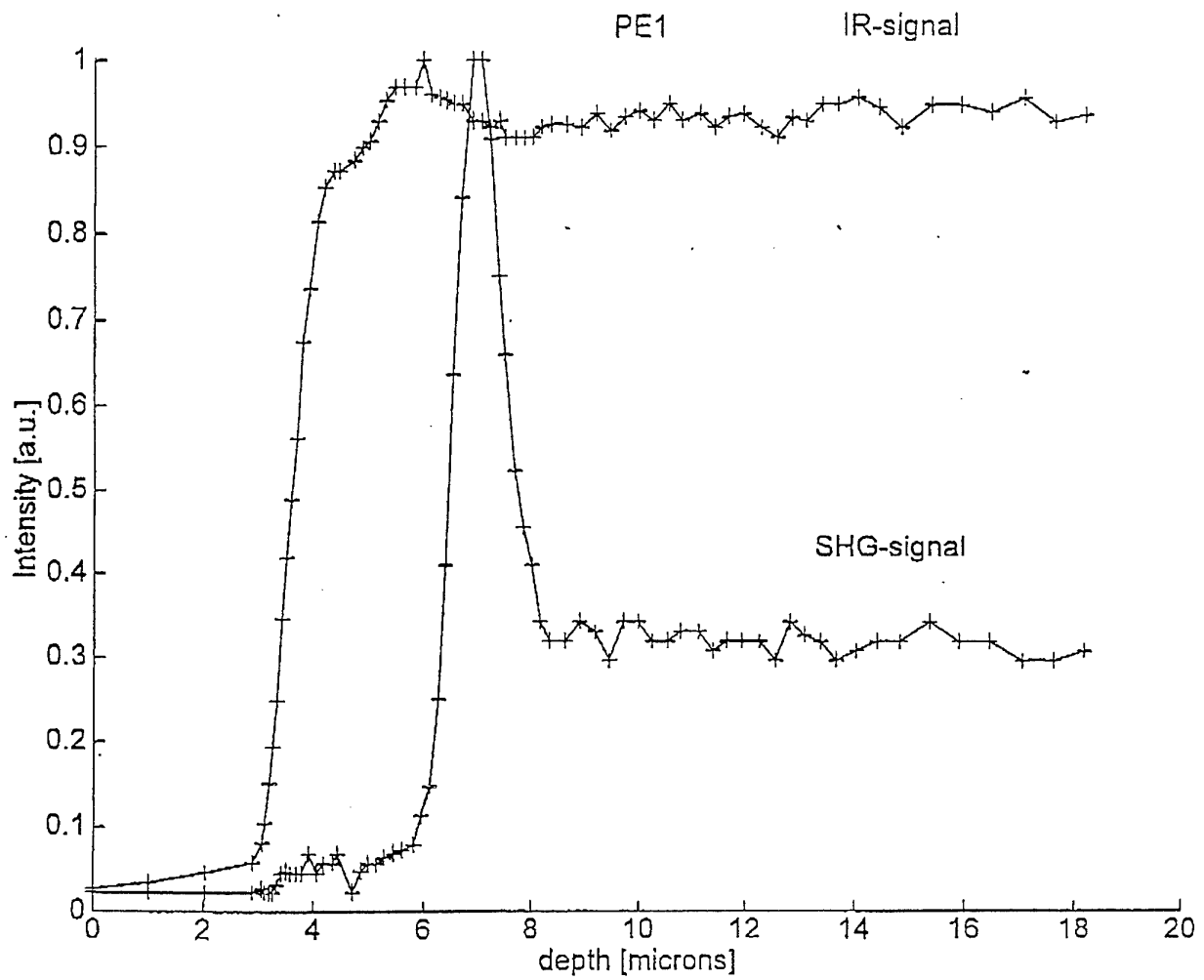
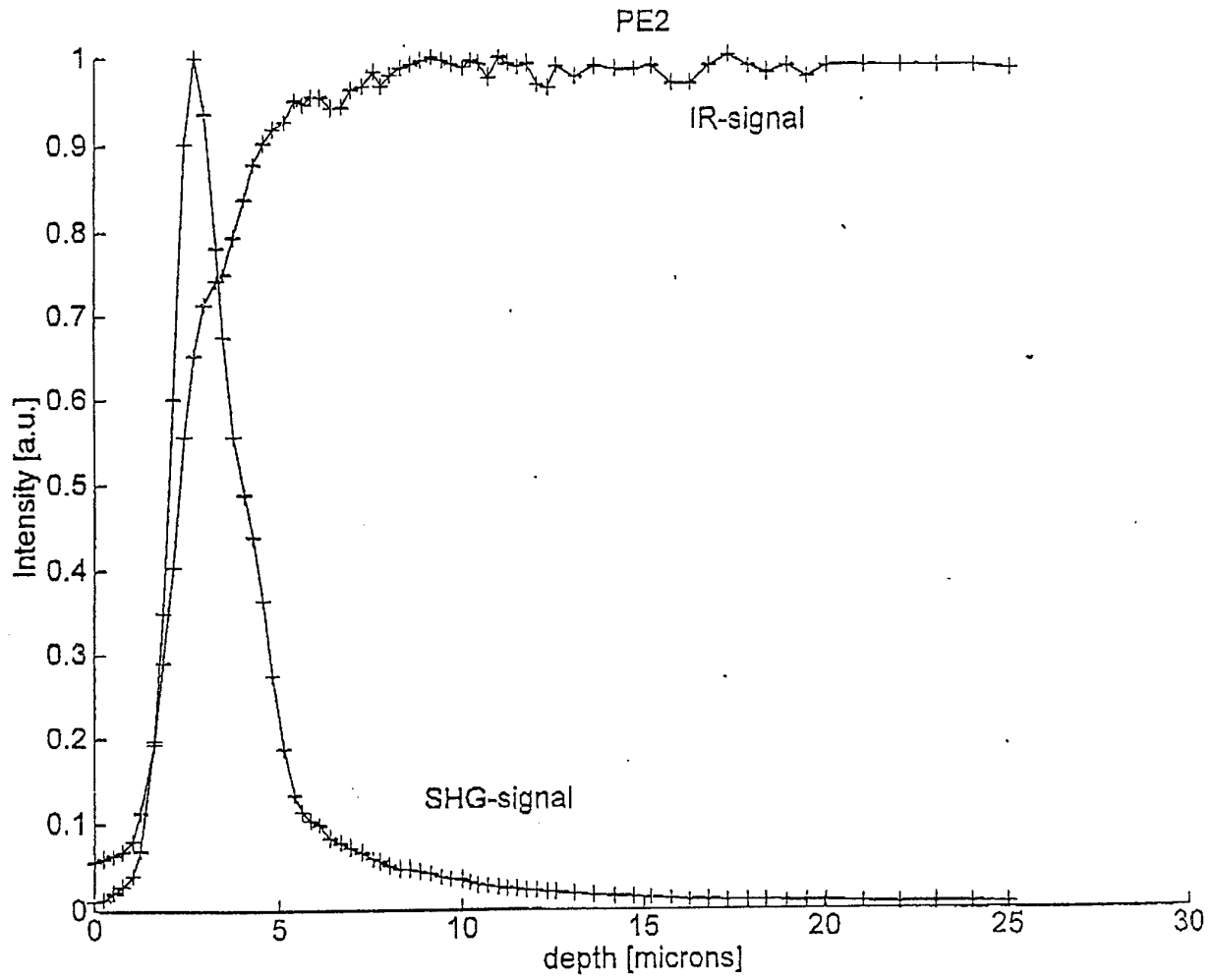


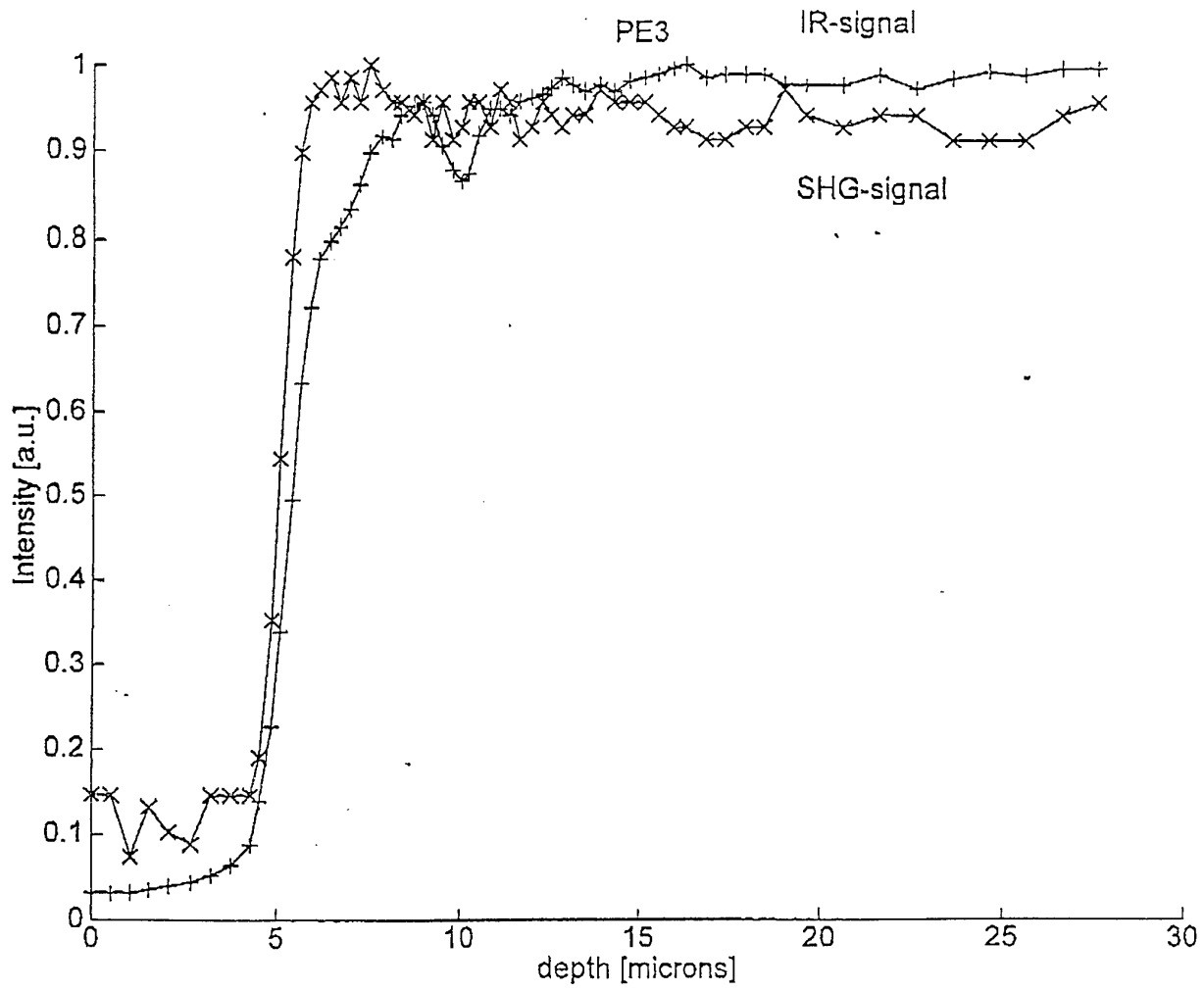
Fig. 29. Experimental set-up used to measure the nonlinear coefficient in the waveguide using the reflected SHG signal.

The results obtained on different sort of PE waveguides are presented in Fig. 30 to Fig 32.

They clearly show that the PE_{III} process does not reduce the nonlinear coefficient. At the contrary, the PE_I process completely destroys the nonlinearity in the exchanged region. Rocking curves will be performed on these particular samples in order to identify the crystallographic phases involved in the reduction of the nonlinear coefficient. These measurements also show a dramatic increase of the SHG signal at the interface between the substrate and the PE_I waveguide and at the surface of the annealed waveguides. This increase can be due to an increase of the nonlinear coefficient in a transition layer, or to high scattering in this layer. The second explanation is more likely to be the right one, but investigations are still in progress to conclude.







III.2. Influence of the Proton Exchanged process on the poling

In this field also, preliminary experiment have demonstrated a great potential.

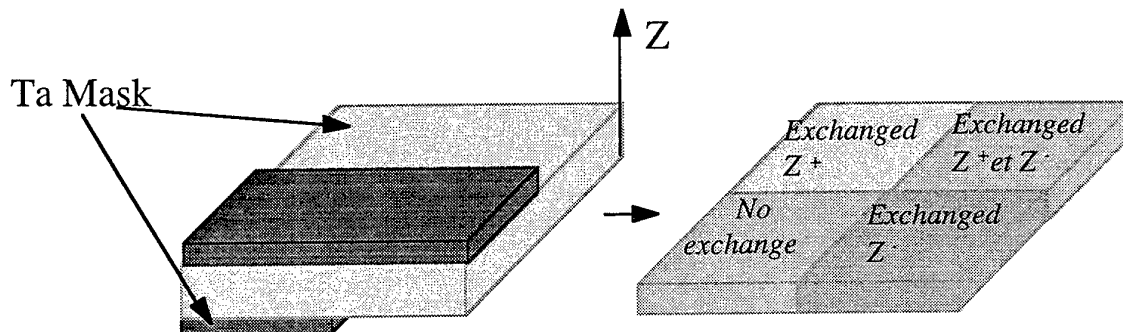
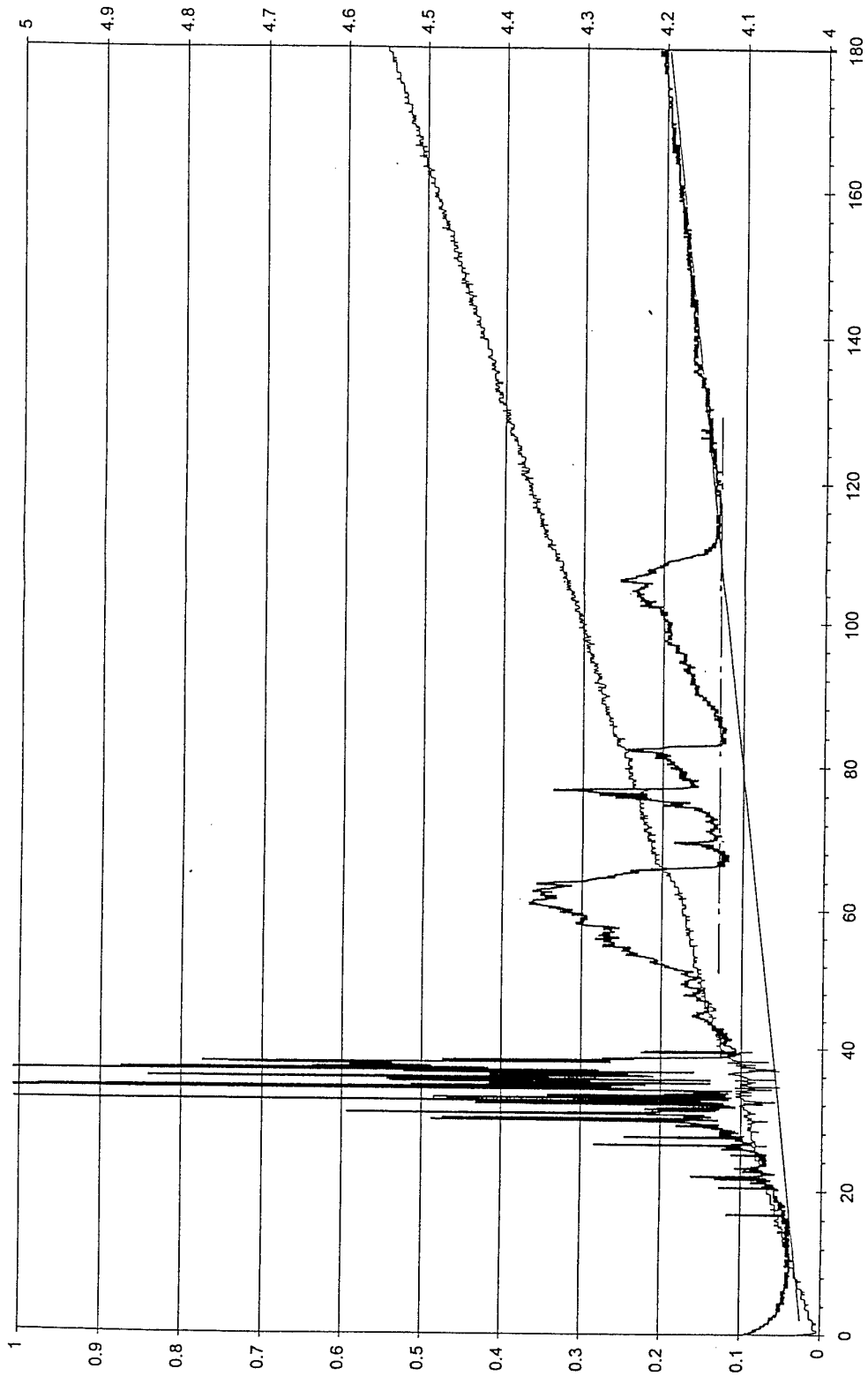


Fig. 34. Masking scheme used to proton exchange a sample in a pyrophosphoric acid bath prior to poling. This allows to define for zones on the crystal

Indeed, doing proton exchange using phosphoric acid and the masking process described in Fig. 34, allows to show that the PE process can significantly modify the poling field of the crystal. In Fig. 35, we plotted the poling current we observed applying a voltage ramp to a sample presenting a 4 μm deep exchange in the uncovered regions. The poling curve clearly presents 4 different current peaks which can be associated to each of the different regions of the sample, the unexchanged region being poled first and the region exchanged on both faces requiring the higher voltage. This has been demonstrated for large areas on the substrate. In order to be able to use this property to pattern the poling, we are now studying the influence of PE using different recipes, and as soon as possible we will apply those recipes to the patterning of the domains.

Poling by ramp; first poling; 4.6-5.2 kV, 180s
Sample hpo42 ; Data hpo42n1



IV. Conclusion

The study we proposed had the objective to establish correlations between the optical properties of the PE waveguides realized on LiNbO_3 and LiTaO_3 , their proton concentrations and their crystalline quality. Indeed these correlations are necessary to determine the optimized fabrication conditions for each of the sophisticated devices combining sources and modulators on the same chip, that can be achieved using these substrates and this technology.

At the end of the first year of the project, and using a first set of samples we have obtained a lot of qualitative results which confirm a certain number of issues such as the fact that the index increase in the PE waveguides is far from proportional to the proton concentration.

We have also verified that the phase diagram established with a completely different equipment and a set of sample of a completely different origin exactly applies to the samples we prepared using benzoic acid melts.

We have identify that the humidity of the melts, if not properly controlled, is an important source of non reproducibility and we are currently developing a set-up allowing a precise control of this parameter.

The first set of sample we produced, indicates that the crystalline quality of the PE layers depends very much on the fabrication parameters. Careful loss measurement will be done to see how this correlates with the propagation losses.

During the second year, and in order to be able to draw new conclusion, we planed to prepare new sets of samples, varying the fabrication parameters in order to have samples presenting PE layers in a given phase, but with different indices. When this is possible, we will also prepare samples presenting the same index profiles by different techniques (direct exchange and exchange followed by annealing for example) and correlate the losses, the proton concentration and the crystallographic organization.

The preliminary results we have indicate that the nonlinear coefficient and the poling possibilities of the LiNbO_3 can be strongly modified by the PE process. During the second year we will use this property to prepare the crystal surface prior to poling and measure the poling parameters as a function of this surface preparation. This should be useful to optimized the fabrication of periodically poled waveguides and to achieve samples with complicated domain shape and sophisticated waveguide design.

References

- ¹ Yu. N. Korkishko et al. *Appl. Opt.* 35 (36), pp. 7056-7060, (1996)
- ² J.M. White and P.F. Heidrich, *Appl. Opt.* 15(1), p. 151-153, (1976)
- ³ J.M. Zavada et al., *J. Appl. Phys.* 77(6), p. 2697, (1995)
H.C. Casey et al. *Appl. Phys. Lett.*, 63(6), p. 718, (1993)

SECONDARY ION MASS SPECTROMETRY ANALYTICAL REPORT

June 10, 1997

Re: Invoice #97-854
Problem #11-7777

Purpose:

To determine the profiles of H and Li in proton-exchanged LiNbO₃ samples.

Experimental Conditions

The analyses were carried out using a PHI 6300 secondary ion mass spectrometer having a quadrupole mass filter. Measurements were accomplished using Cs⁺ primary ion bombardment with positive secondary ion detection. An electron gun was used to bombard the samples during profiling to compensate for sample charging induced by ion bombardment.

Quantification:

Quantification of the profiles is accomplished by using relative sensitivity factors determined by analyzing, along with your samples, a characterized proton-exchanged LiNbO₃ sample. This standard has been previously characterized by SIMS and HFS (Hydrogen Forward Scattering) measurements. The HFS measurement shows that in the proton-exchanged region there is complete exchange of H for Li. Therefore the amount of H in this region is 20 atomic percent. I have used this standard to calibrate the H profiles. The Li profiles are calibrated by setting the flat part of the profile in the substrate equal to a value of 2.89×10^{22} atoms/cm³, the ideal atom density for the phase LiNbO₃. Because most LiNbO₃ is grown at the minimum melt composition, this value is not strictly accurate, however we do not have a good way to accurately measure the absolute Li content of the substrates. Profiles of the standards are enclosed for your information. Based on previous repeat analyses of proton-exchanged LiNbO₃, the calculated concentrations are accurate to within 25%.

The depth scales are calibrated after the analyses by measuring, with a stylus profilometer, the depth of the craters sputtered into your samples. Plotting the profiles using the total crater depth assumes that the sputtering rate is constant within the profile. This may not be true for exchanged samples having a step gradient, because the high H content of the exchange layer decreases the sputtering rate. However for the step gradient samples we have sputtered very little into the unexchanged substrate, so the crater measurement calibrates the sputtering rate of the exchanged region accurately. For the annealed samples having a gradient profile, there is little effect on the sputtering rate because the amount of H is relatively low compared to Li. For 8 of your samples measured in a single run during these analyses, the sputtering rates show a relative standard deviation of 0.8%. This is for both gradient and step samples. Therefore, we appear to have very similar sputtering rates for all of your samples regardless of their structure. I have found from previous measurements that the sputtering rate does not vary significantly within the proton-exchanged region.

Results:

Figures 1-12 give plots of the PROCESSED (concentration versus depth) profiles acquired on your samples. Figures 11 and 12 are profiles of the standards.

The results show a variety of profiles that appear to correlate with the different phases you have observed using X-ray analysis. For the phases α , κ_1 and κ_2 there is an increasing amount of H in the near surface region that correlates with increasing refractive index. For samples β_1 and β_2 there are less clear

compositional differences. However the two β_1 samples appear to have more Li within the proton-exchange region, on average, than the β_2 samples.

A disk containing ASCII data is enclosed for your use. I hope these results are of use to you in your process development. As I am sure you will have questions about the results presented in this report, please feel free to contact me by phone, FAX or e-mail. Please let us know if we can be of service to you in the future concerning your materials characterization needs.



Steven W. Novak, Ph.D.
Manager, Dynamic SIMS Services
email:snovak@evanseast.com

PROCESSED DATA
18 Apr 97

Evans East
FILE: 9785416

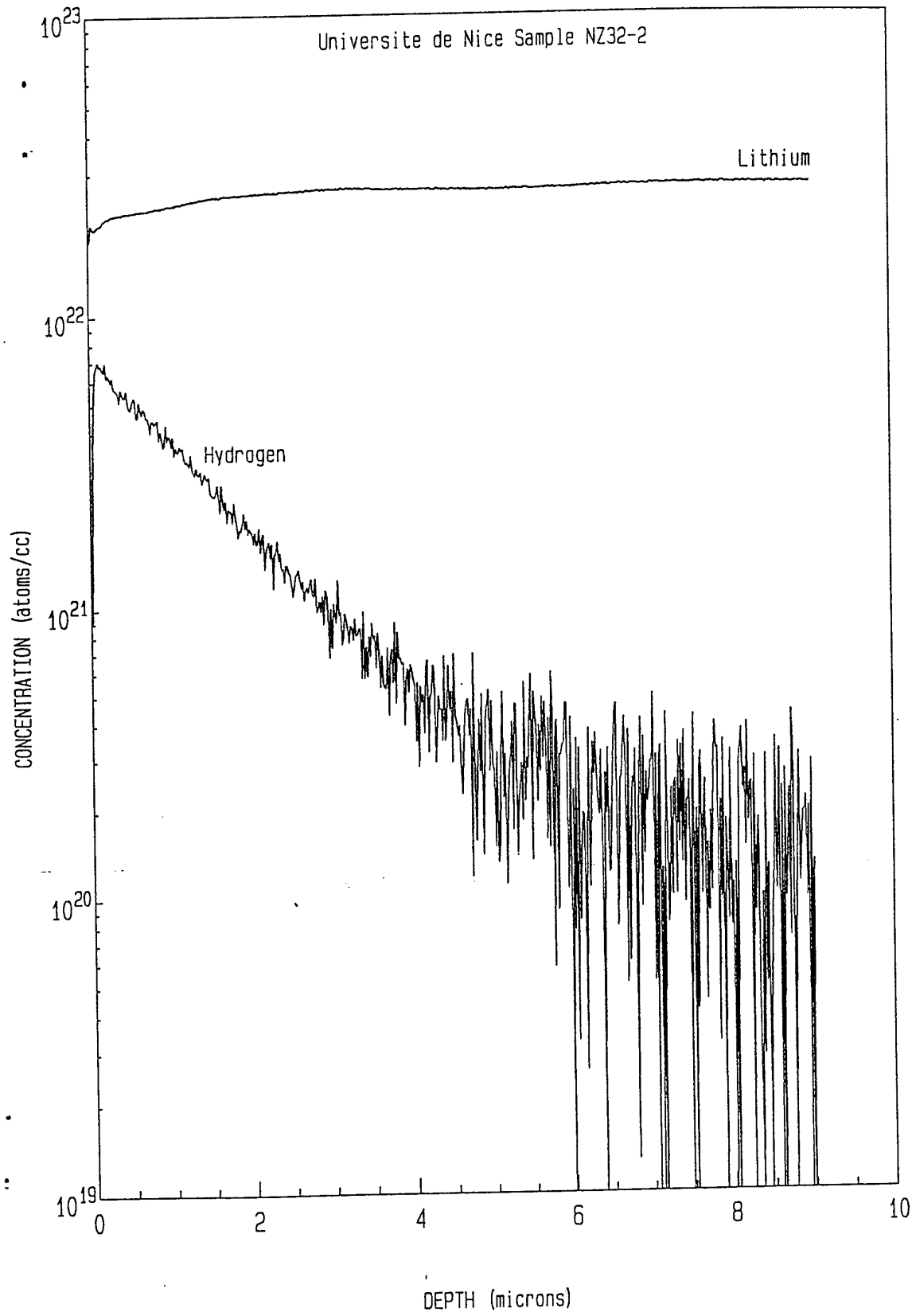


Fig. 1

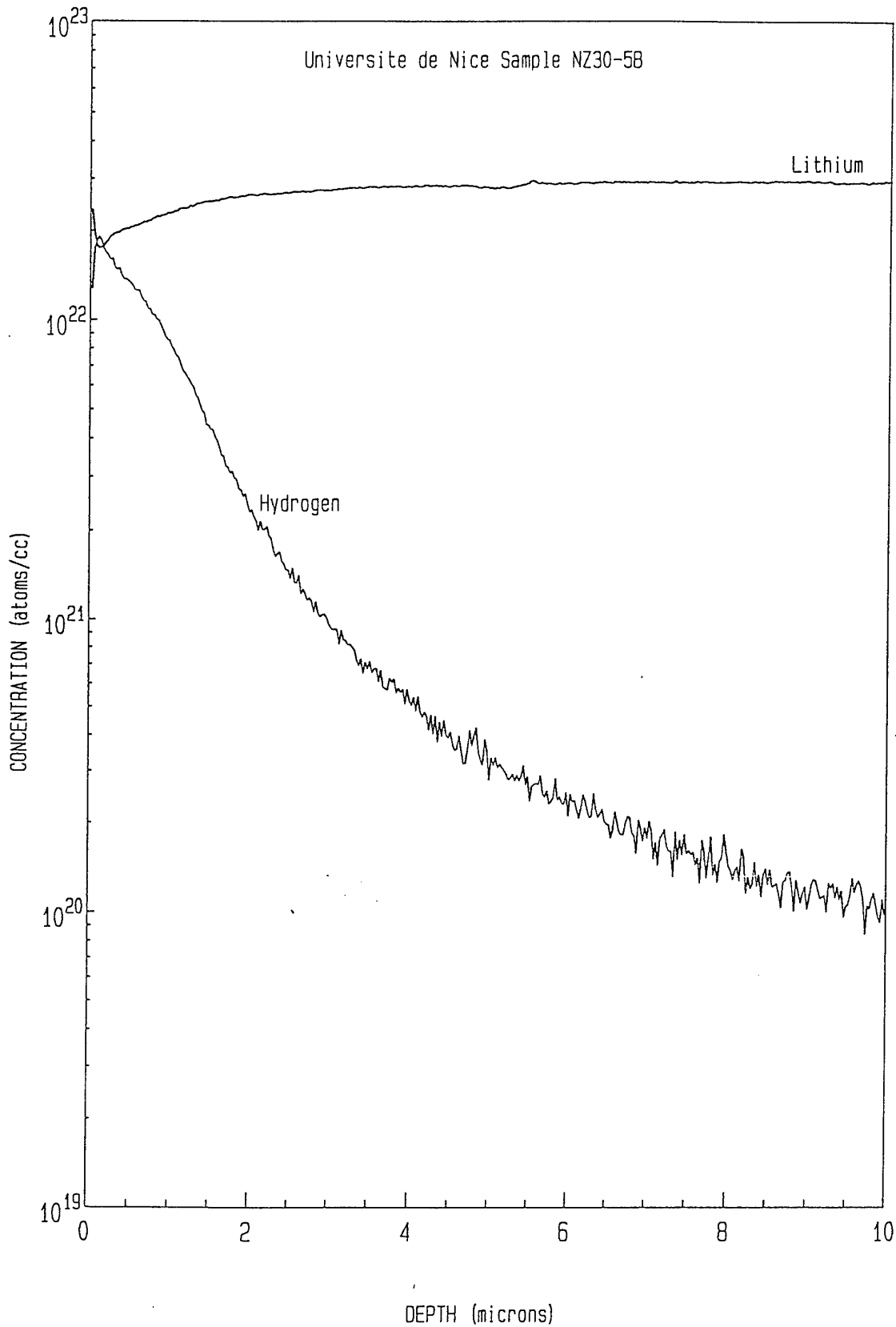


Fig. 2

PROCESSED DATA
18 Apr 97

Evans East
FILE: 9785415

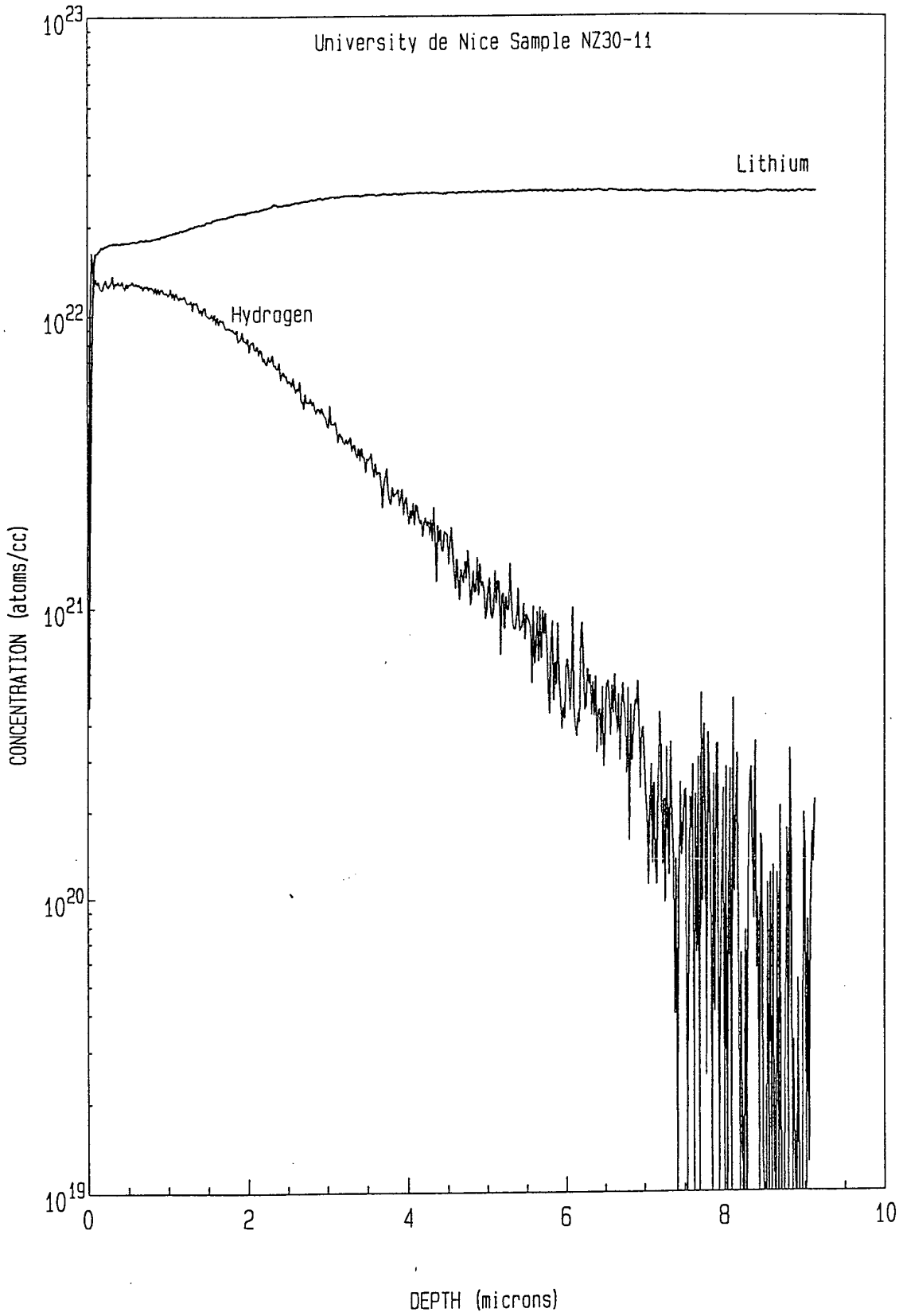


Fig. 3

PROCESSED DATA
18 Apr 97

Evans East
FILE: 31-3ovr

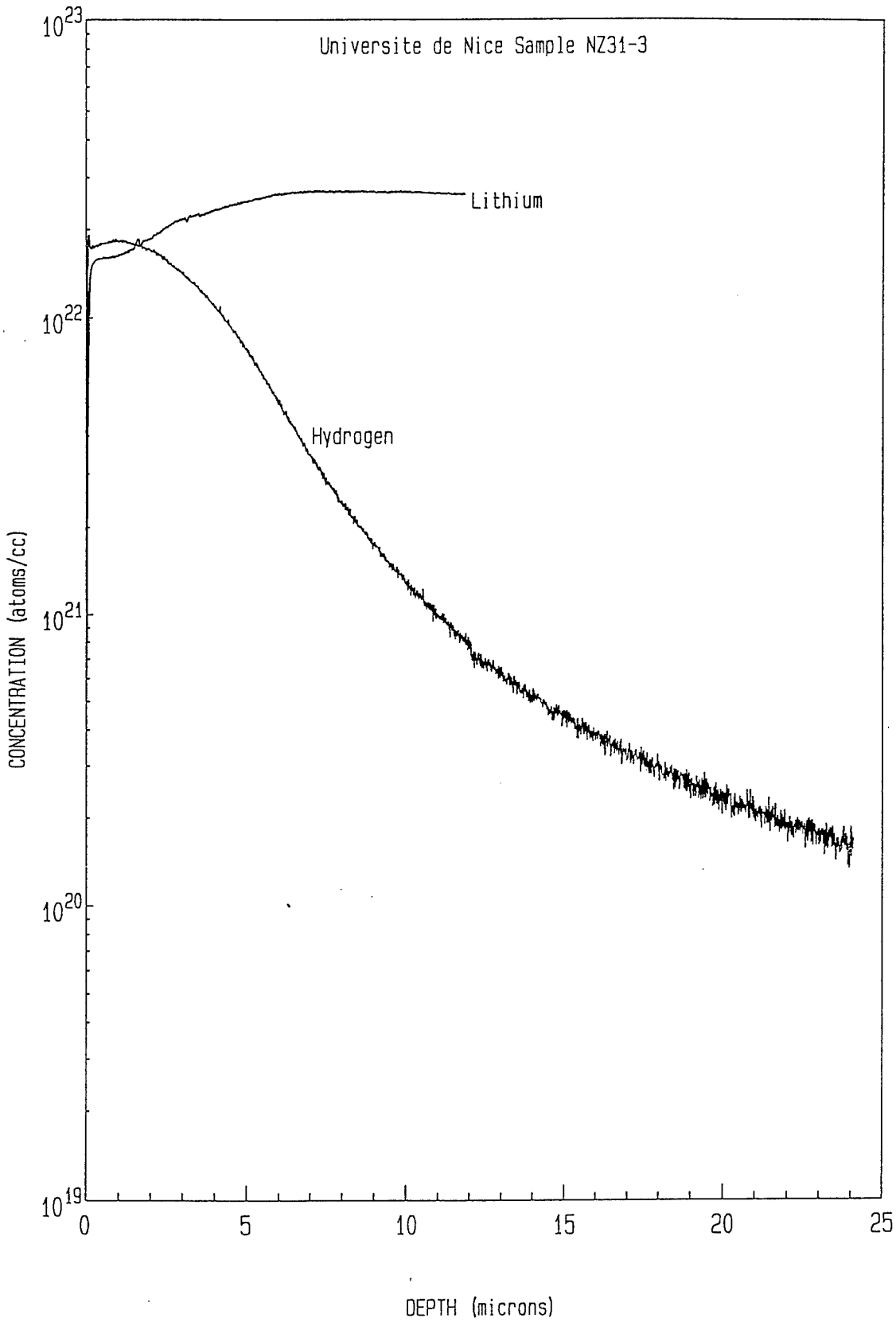


Fig. 4

PROCESSED DATA

6 May 97

Evans East

FILE: 7100432

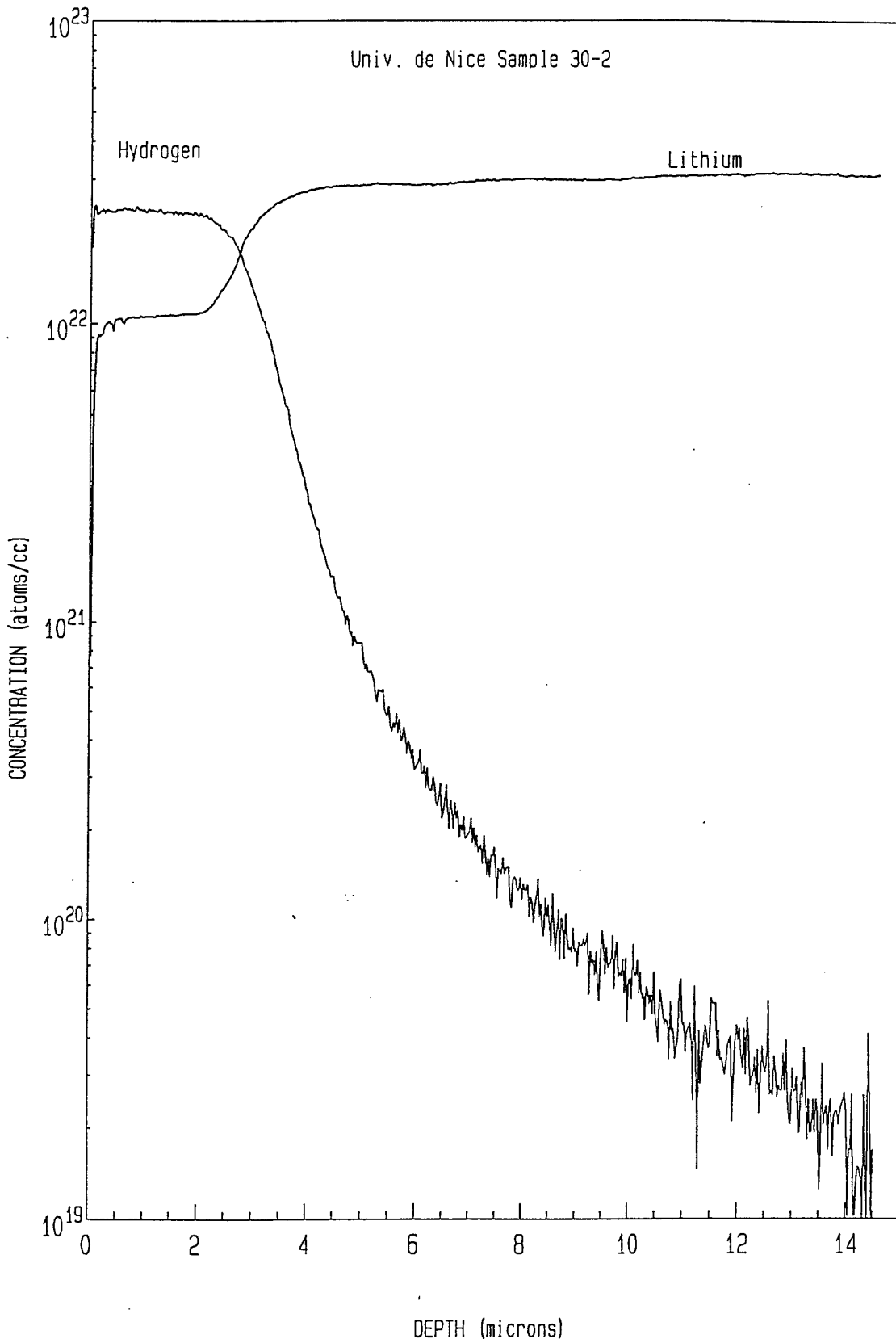


Fig. 5

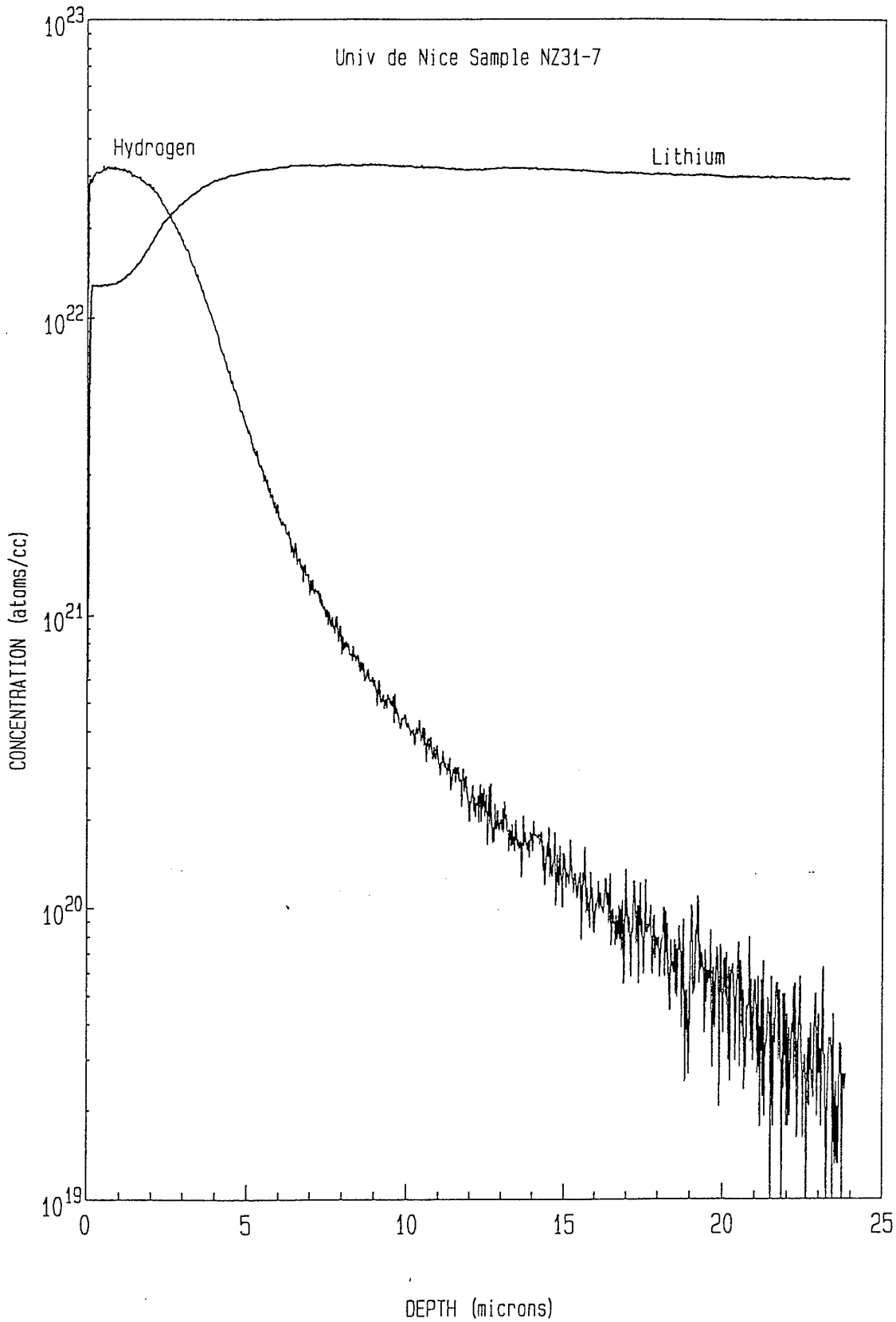


fig.6

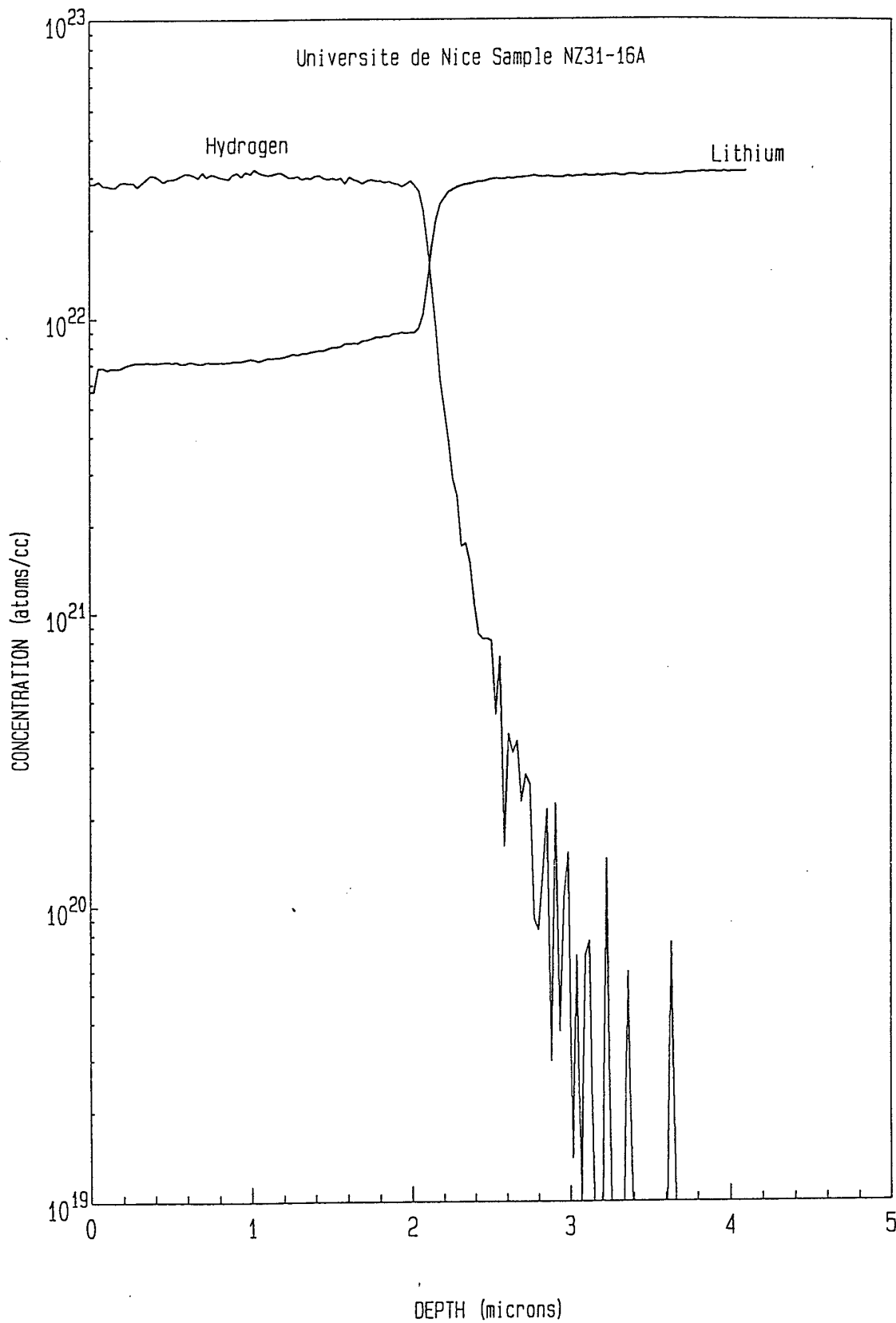


Fig. 7

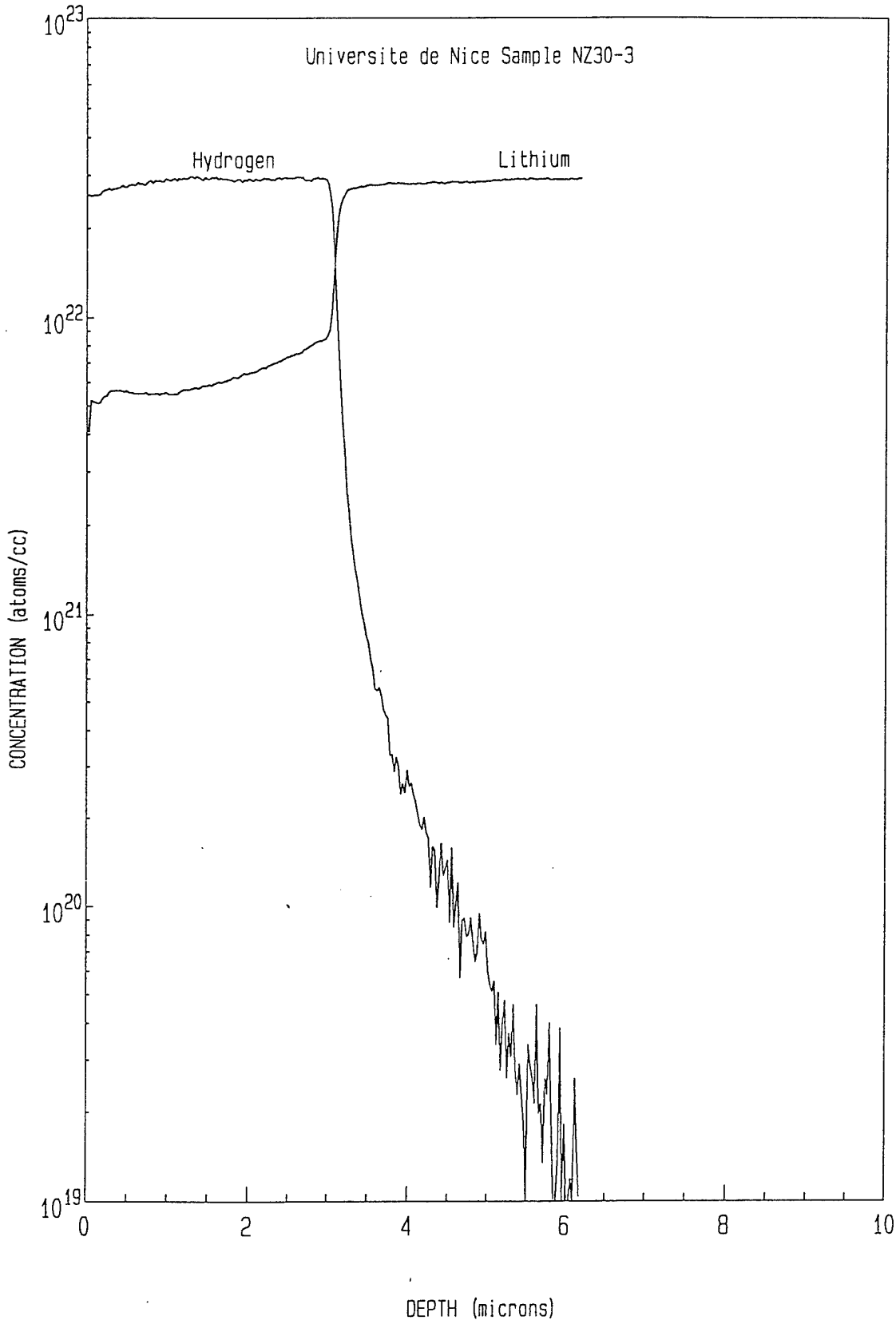


Fig 8

PROCESSED DATA

18 Apr 97

Evans East

FILE: 9785412

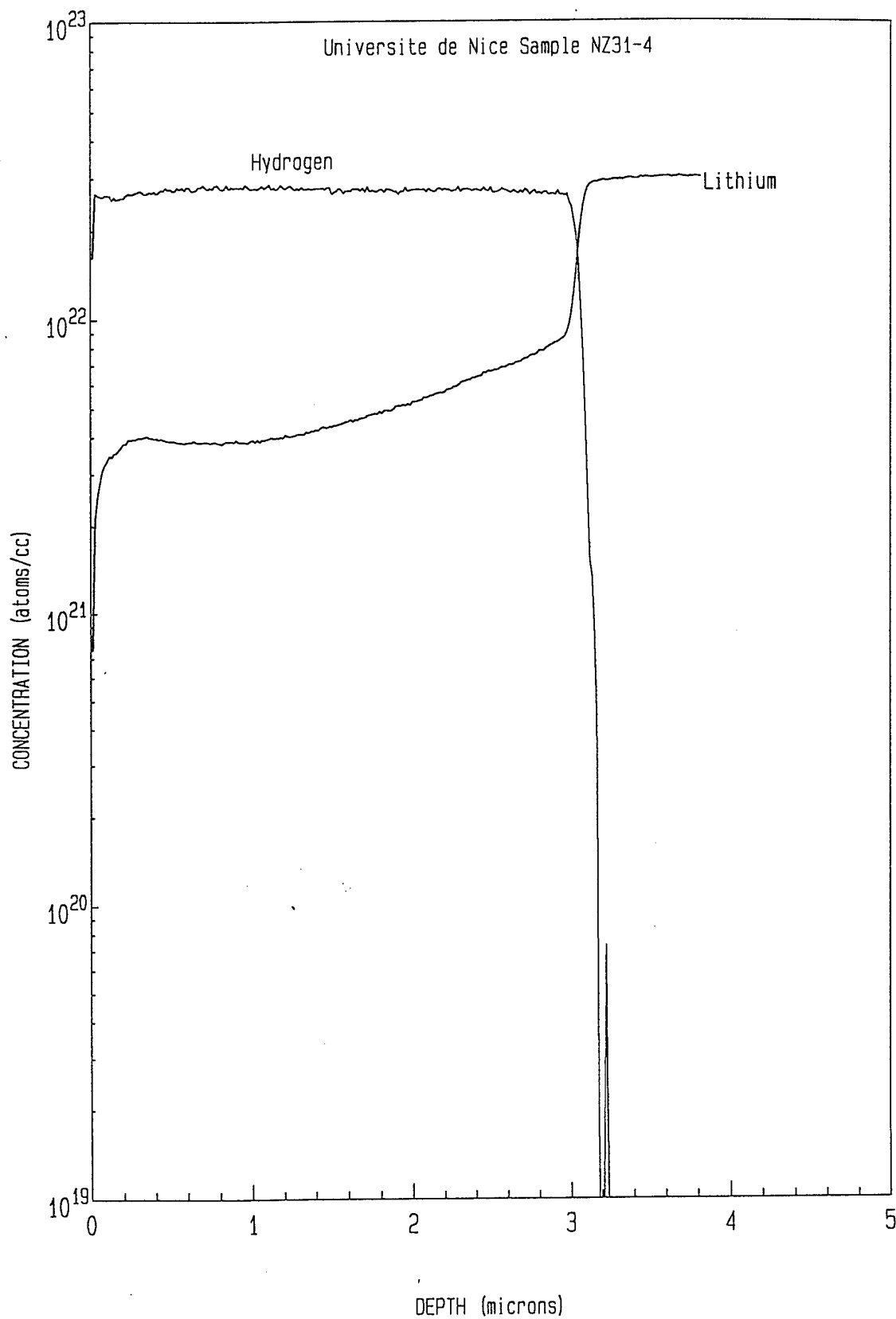


Fig. 9

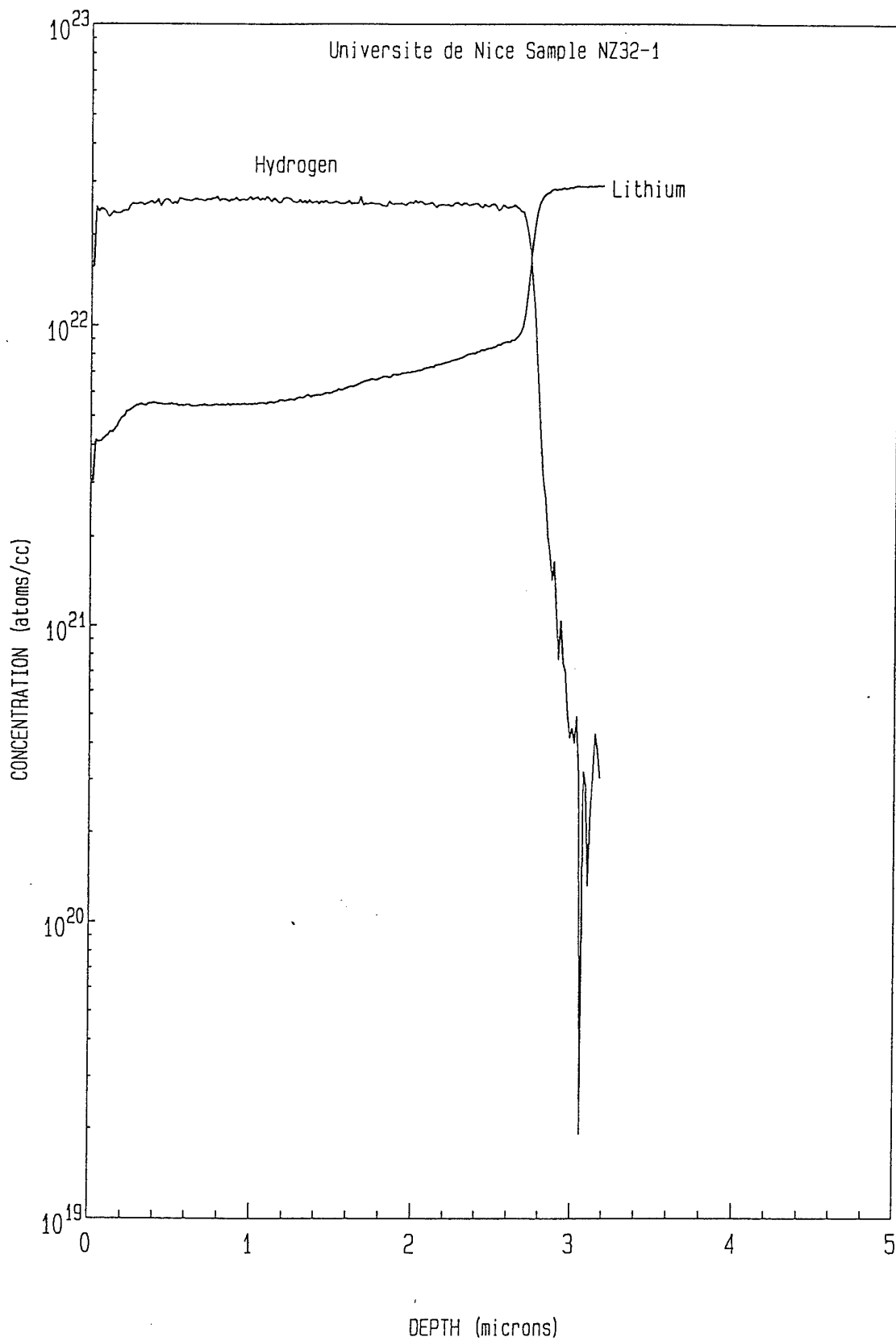


Fig. 10

PROCESSED DATA

6 May 97

Evans East

FILE: 7100433

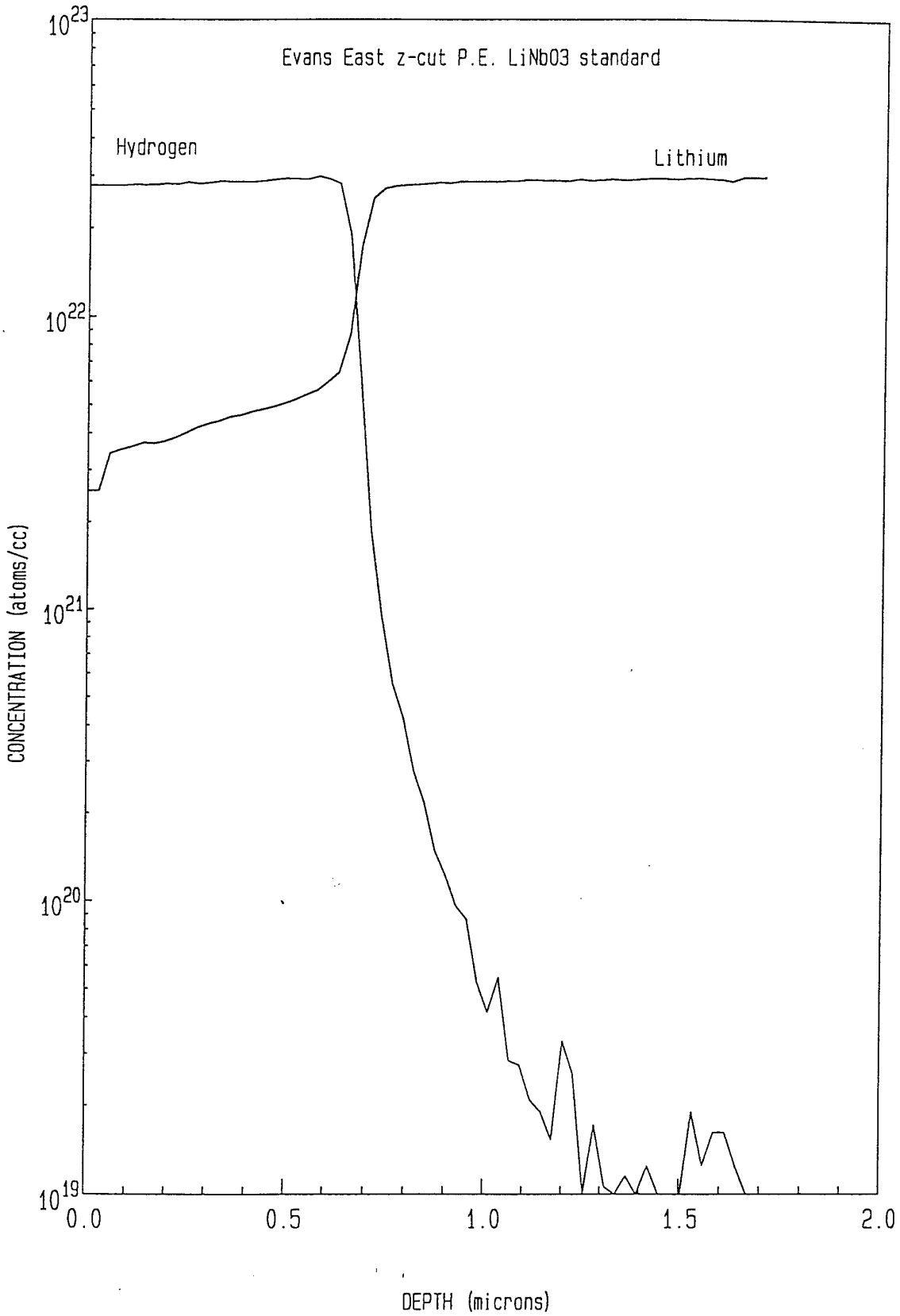


Fig. 11

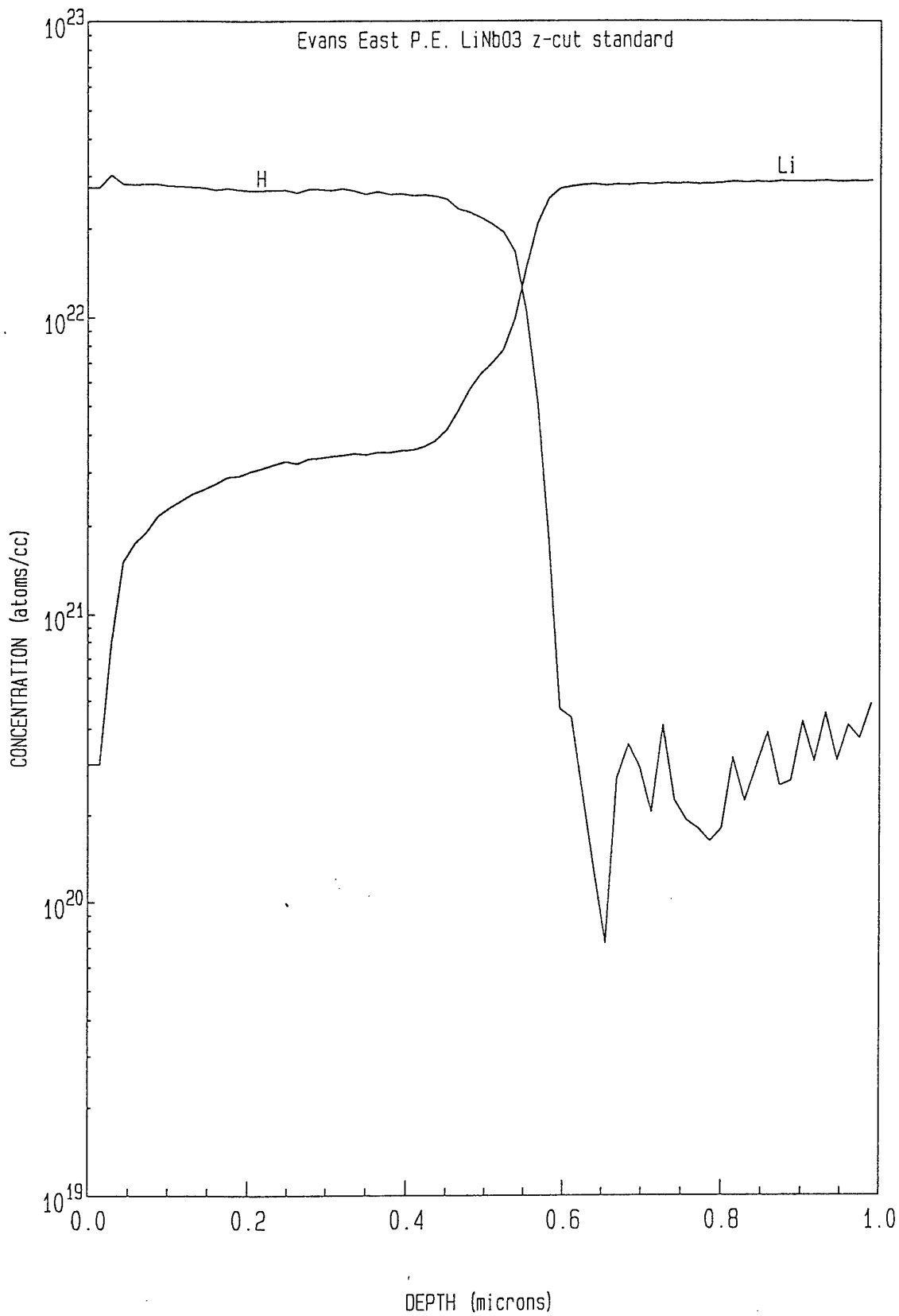


Fig. 12